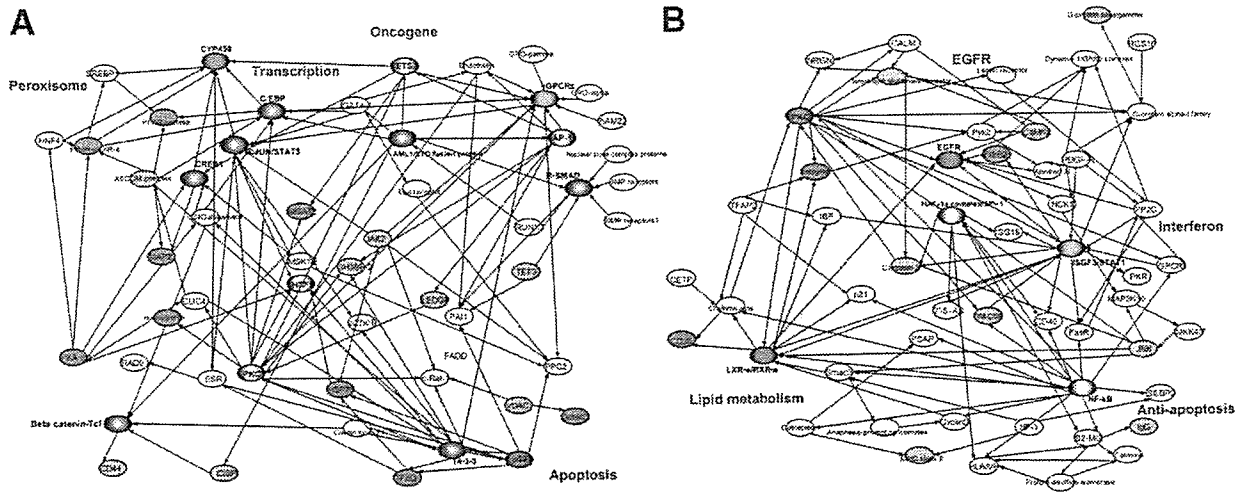

Fig. 5. (A) Gene network of differentially expressed genes in CH-B. (B) Gene network of differentially expressed genes in CH-C. Core transcription factors are represented by black ovals. Green ovals show genes expressed predominantly in hepatocytes and blue ovals show genes expressed predominantly in lymphocytes.

family were induced by several transcriptional factors including AP-1, c-fos, and STAT3, which were all strongly upregulated. In CH-C, inflammation-related angiogenic factors such as IL-8, IL-18, and PDGF1, induced by NF-κB, were also upregulated (Fig. 6B, Fig. 7). Thus, CH-B and CH-C showed different angiogenic properties, which implied that the tumorigenic process in CH-B and CH-C may differ.

Table 7. Transcription Regulation

	Frequent pathway process	*P* value
	Chronic hepatitis B	
1	Mothers against decapentaplegic homolog 3 (SMAD3)	5.25E-36
2	Activator protein-1 (AP-1)	4.24E-33
3	p53	8.49E-33
4	cAMP-responsive element binding protein 1 (CREB1)	2.39E-32
5	v-ets erythroblastosis virus E26 oncogene homolog 1 (ETS1)	3.38E-32
6	Sterol regulatory element binding transcription factor 1 (SREBP1)	6.73E-32
7	Transcription factor binding to IGHM enhancer 3 (TFE3)	9.48E-32
8	Signal transducer and activator of transcription 3 (STAT3)	1.33E-31
9	v-ets erythroblastosis virus E26 oncogene homolog 2 (ETS2)	1.88E-31
10	Transcription factor 7/Lymphoid enhancer binding factor 1 [Tcf(ref)]	1.88E-31
	Chronic hepatitis C	
1	Nuclear factor of κ light polypeptide gene enhancer in B-cells 1 (NF-κB)	1.32E-35
2	Interferon regulatory factor 1 (IRF1)	4.34E-33
3	Splicing factor 1(SF1)	9.17E-33
4	Signal transducer and activator of transcription 1 (STAT1)	1.28E-32
5	Retinoid acid receptor- (RAR)	1.81E-32
6	Nuclear factor of κ light polypeptide gene enhancer in B-cells 2 (RelA)	3.56E-32
7	Vitamin D receptor (VDR)	5.00E-32
8	Wilms tumor 1(WT1)	7.02E-32
9	Sterol regulatory element binding transcription factor 2 (SREBP2)	9.84E-32
10	Epidermal growth factor receptor (EGFR)	1.92E-31

Quantitative RTD-PCR. We performed quantitative real-time detection PCR (RTD-PCR) using 15 Taq-Man probes. The results of RTD-PCR on whole liver biopsy and LCM samples are shown in Fig. 7. In CH-B, apoptosis-inducing genes such as CASP9, IFNG, GZMA, TP53, BGA2, and DIABLO were upregulated. In CH-C, IFN-α-induced genes and chemokines such as MxA, IFI15, OAS2, and IP10 were upregulated. Angiogenic factors such as FGFB, ANGPT1, and VEGF were upregulated in CH-B, and another angiogenic factor, PDECGF, was upregulated in CH-C. The results are consistent with those from the cDNA microarray.

Discussion

The biological activity of viral coding polyproteins of HBV and HCV has been extensively investigated in cell lines and in transgenic mouse models. For example, accumulated evidence shows HBV-X protein to be a transcriptional transactivator that interacts with p53 tumor suppressor protein, modulating its signaling pathway.[9,25] The transgenic mouse model with overexpression of HCV polyproteins in the liver develops steatosis and HCC.[26,27] However, these findings have not been well evaluated in clinical samples.

Using in-house cDNA microarray analysis of 1080 genes, we previously reported differing gene expression profiles of liver tissue from patients with CH-B and CH-C.[13] However, the detailed signaling pathways underlying these diseases needed further clarification. In this study,

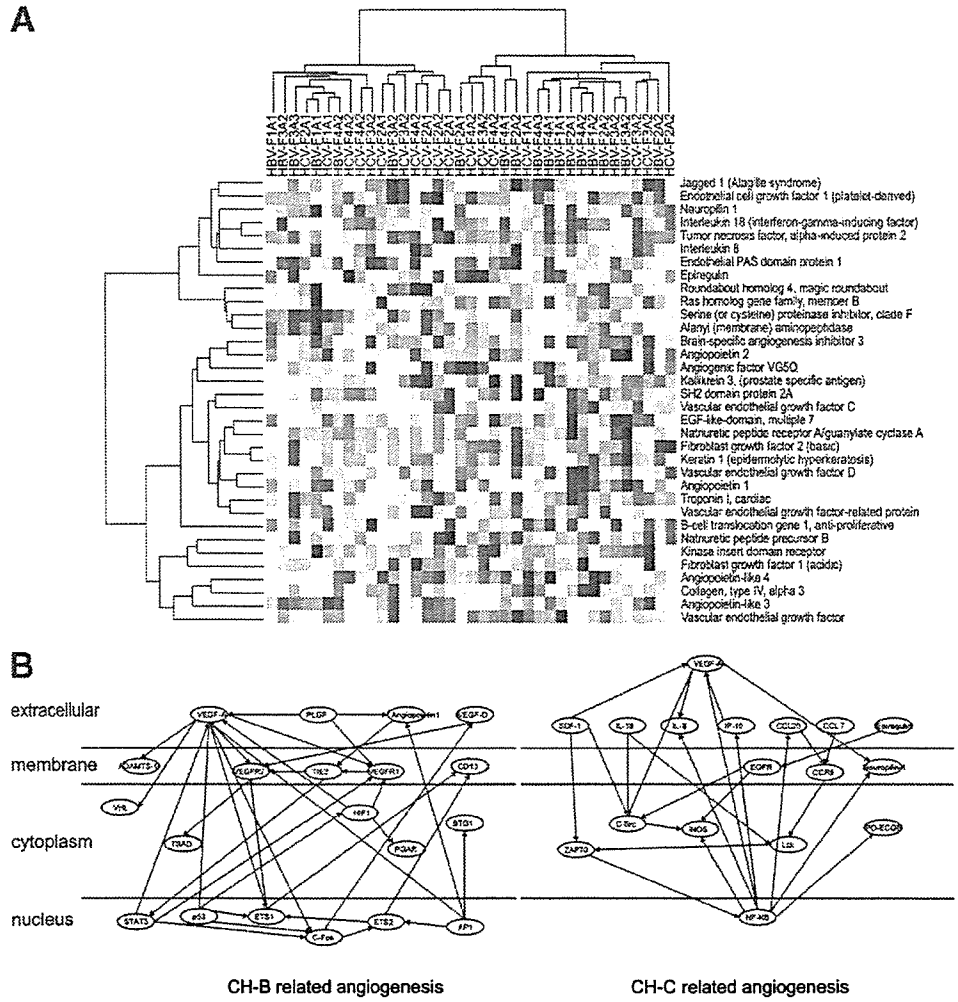

Fig. 6. (A) Hierarchical clustering of whole liver samples using angiogenic genes. (B) Gene network of angiogenic genes in CH-B and CH-C.

we constructed a new microarray slide, liver chip 10 K, consisting of 9614 clones which were selected from unique tag sequences in our hepatic SAGE libraries, including 667,067 tag sequences (manuscript in preparation), for the purpose of analyzing gene expression profiling in liver disease. We analyzed the gene expression profiles of whole liver biopsy specimens obtained from 37 patients with CH-B and CH-C. In addition, we selectively isolated liver-infiltrating lymphocytes (16 samples) and hepatocytes (8 samples) from liver biopsy specimens using LCM (Fig. 1D) and analyzed their gene expression. Furthermore, SAGE data were obtained from pooled samples of 3 CH-B or 3 CH-C patients, and their gene expression data were integrated to reveal the comprehensive, detailed gene network involved in CH-B and CH-C, respectively.

Hierarchical clustering analysis of 37 patients grouped these patients into 2 groups with CH-B or CH-C, with a few exceptions. Moreover, gene prediction analysis significantly discriminated between CH-B and CH-C patients ($P < .001$). HBV or HCV was the only factor significantly involved in patient classification, and other factors such as histological stage, disease activity, age, and ALT levels were not significantly associated with the classification of these patients. This indicates that virus type, whether HBV or HCV, influences liver gene expression to a greater degree than any other clinical parameter, such as degree of fibrosis or inflammation (Table 2).

The pathway analysis and GO comparison in CH-B and CH-C using whole liver biopsy revealed that antigen-presenting genes, IFN-α-induced genes, G_1/S transition genes, and cholesterol biosynthesis and platelet-derived factors were upregulated in CH-C, whereas genes related to cell death, DNA repair, and peroxisomes were upregulated in CH-B (Tables 5-6, Fig. 3). The association of HCV infection with steatosis in the liver in CH-C has

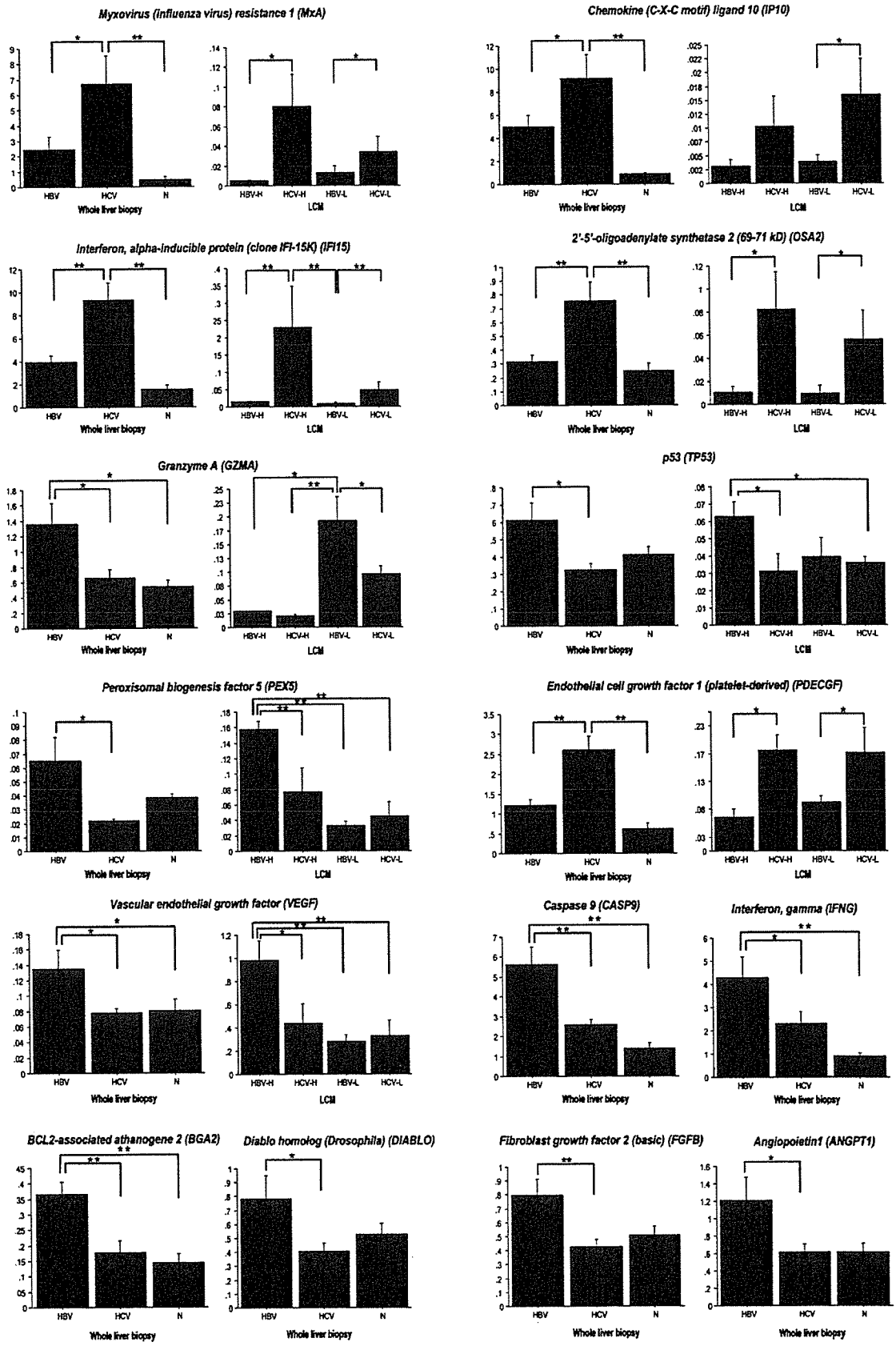

Fig. 7. Quantitative real-time detection PCR (RTD-PCR) using 15 TaqMan probes. The results of whole liver biopsy (HBV; 19 samples of CH-B, HCV; 18 samples of CH-C and N; 6 samples of normal liver) and LCM samples (HBV-H; 4 samples of hepatocyte in CH-B, HCV-H; 4 samples of hepatocyte in CH-C, HBV-Ly; 8 samples of lymphocyte in CH-B, HCV-Ly; 8 samples of lymphocyte in CH-C) were shown. $*P < .05$, $**P < .01$.

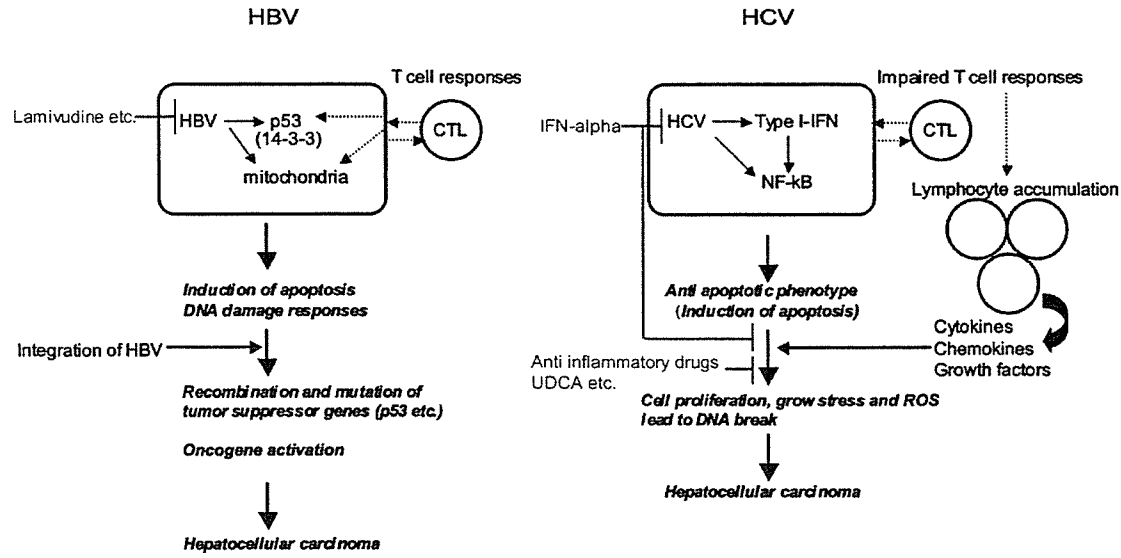

Fig. 8. Schematic representation of different pathogenesis of hepatitis and development of HCC in CH-B and CH-C.

been reported.[28,29] There might also be an association between HBV replication and peroxisomal activation, as reported using hepatoma-derived cell lines.[30,31] We combined SAGE data with those from cDNA microarray analysis and constructed the detailed and comprehensive gene network underlying CH-B and CH-C. In CH-B, p53-mediated and 14-3-3-mediated pro-apoptotic signaling; transcription factors such as AP-1, C/EBP, c-JUN, and CREB1; and oncogenes and peroxisomes were activated (Fig. 5). In CH-C, type 1-IFN (ISGF3/STAT1), NF-κB, EGFR, and LXR/RXR signaling were activated.

Lesion-specific gene expression analysis by LCM revealed more precise differences in gene expression between CH-B and CH-C (Fig. 4, Fig. 7), although a larger number of samples will be needed to reach concrete conclusions. Interestingly, many IFN-α-induced genes were upregulated in hepatocytes, but not in lymphocytes, in CH-C. On the other hand, DNA repair genes such as p53 and RAD were induced in hepatocytes in CH-B. Detailed analysis of lymphocyte markers revealed Th1-dominant responses in the liver in CH-B and Th2-dominant responses in the liver in CH-C.

Despite greater lymphocyte infiltration and homing in the liver, a weak T cell response and no T cell accumulation were observed in CH-C.[32,33] These contributed to the induction of various chemokines, cytokines, and growth factors, which may lead to cell proliferation and angiogenesis in CH-C. Surprisingly, gene expression profiling of angiogenic factors revealed clear differences in CH-B and CH-C. Many of the chemokines involved in angiogenesis are independent of VEGF-mediated or angiopoietin-mediated signaling pathways.[34] These findings possibly reflect a different means of carcinogenesis of HCC in CH-B and CH-C (Fig. 6).

In summary, we investigated the detailed signaling pathways in CH-B and CH-C. Although our data reveal the different signaling pathways induced in CH-B and CH-C, the precise mechanisms underlining these differences must be proven experimentally in the future. Nevertheless, from the therapeutic point of view, these results might be indicative that antiviral agents will be most effective for CH-B whereas anti-inflammatory drugs, other than IFN, would be effective for CH-C, for the prevention of HCC (Fig. 8). Further studies are needed to elucidate these findings clinically and biologically.

Acknowledgment: We thank Masami Ueda and Mikiko Nakamura for excellent technical assistance.

References

1. Shafritz DA, Shouval D, Sherman HI, Hadziyannis SJ, Kew MC. Integration of hepatitis B virus DNA into the genome of liver cells in chronic liver disease and hepatocellular carcinoma. Studies in percutaneous liver biopsies and post-mortem tissue specimens. N Engl J Med 1981;305:1067-1073.
2. Choo QL, Kuo G, Weiner AJ, Overby LR, Bradley DW, Houghton M. Isolation of a cDNA clone derived from a blood-borne non-A, non-B viral hepatitis genome. Science 1989;244:359-362.
3. Kiyosawa K, Sodeyama T, Tanaka E, Gibo Y, Yoshizawa K, Nakano Y, et al. Interrelationship of blood transfusion, non-A, non-B hepatitis and hepatocellular carcinoma: analysis by detection of antibody to hepatitis C virus. HEPATOLOGY 1990;12:671-675.
4. Huang HP, Tsuei DJ, Wang KJ, Chen YL, Ni YH, Jeng YM, et al. Differential integration rates of hepatitis B virus DNA in the liver of children with chronic hepatitis B virus infection and hepatocellular carcinoma. J Gastroenterol Hepatol 2005;20:1206-1214.

5. Minami M, Daimon Y, Mori K, Takashima H, Nakajima T, Itoh Y, et al. Hepatitis B virus-related insertional mutagenesis in chronic hepatitis B patients as an early drastic genetic change leading to hepatocarcinogenesis. Oncogene 2005;24:4340-4348.
6. Kim CM, Koike K, Saito I, Miyamura T, Jay G. HBx gene of hepatitis B virus induces liver cancer in transgenic mice. Nature 1991;351:317-320.
7. Murakami S, Cheong JH, Kaneko S. Human hepatitis virus X gene encodes a regulatory domain that represses transactivation of X protein. J Biol Chem 1994;269:15118-15123.
8. Murakami S, Cheong J, Ohno S, Matsushima K, Kaneko S. Transactivation of human hepatitis B virus X protein, HBx, operates through a mechanism distinct from protein kinase C and okadaic acid activation pathways. Virology 1994;199:243-246.
9. Lin Y, Nomura T, Yamashita T, Dorjsuren D, Tang H, Murakami S. The transactivation and p53-interacting functions of hepatitis B virus X protein are mutually interfering but distinct. Cancer Res 1997;57:5137-5142.
10. Yasui K, Wakita T, Tsukiyama-Kohara K, Funahashi SI, Ichikawa M, Kajita T, et al. The native form and maturation process of hepatitis C virus core protein. J Virol 1998;72:6048-6055.
11. Hsieh TY, Matsumoto M, Chou HC, Schneider R, Hwang SB, Lee AS, et al. Hepatitis C virus core protein interacts with heterogeneous nuclear ribonucleoprotein K. J Biol Chem 1998;273:17651-17659.
12. Colombari R, Dhillon AP, Piazzola E, Tomezzoli AA, Angelini GP, Capra F, et al. Chronic hepatitis in multiple virus infection: histopathological evaluation. Histopathology 1993;22:319-325.
13. Honda M, Kaneko S, Kawai H, Shirota Y, Kobayashi K. Differential gene expression between chronic hepatitis B and C hepatic lesion. Gastroenterology 2001;120:955-966.
14. Desmet VJ, Gerber M, Hoofnagle JH, Manns M, Scheuer PJ. Classification of chronic hepatitis: diagnosis, grading and staging. HEPATOLOGY 1994;19:1513-1520.
15. Shirota Y, Kaneko S, Honda M, Kawai HF, Kobayashi K. Identification of differentially expressed genes in hepatocellular carcinoma with cDNA microarrays. HEPATOLOGY 2001;33:832-840.
16. Kawai HF, Kaneko S, Honda M, Shirota Y, Kobayashi K. Alpha-fetoprotein-producing hepatoma cell lines share common expression profiles of genes in various categories demonstrated by cDNA microarray analysis. HEPATOLOGY 2001;33:676-691.
17. Kawaguchi K, Honda M, Yamashita T, Shirota Y, Kaneko S. Differential gene alteration among hepatoma cell lines demonstrated by cDNA microarray-based comparative genomic hybridization. Biochem Biophys Res Commun 2005;329:370-380.
18. Honda M, Kawai H, Shirota Y, Yamashita T, Kaneko S. Differential gene expression profiles in stage I primary biliary cirrhosis. Am J Gastroenterol 2005;100:2019-2030.
19. Honda M, Kawai H, Shirota Y, Yamashita T, Takamura T, Kaneko S. cDNA microarray analysis of autoimmune hepatitis, primary biliary cirrhosis and consecutive disease manifestation. J Autoimmun 2005;25:133-140.
20. Yamashita T, Hashimoto S, Kaneko S, Nagai S, Toyoda N, Suzuki T, et al. Comprehensive gene expression profile of a normal human liver. Biochem Biophys Res Commun 2000;269:110-116.
21. Yamashita T, Kaneko S, Hashimoto S, Sato T, Nagai S, Toyoda N, et al. Serial analysis of gene expression in chronic hepatitis C and hepatocellular carcinoma. Biochem Biophys Res Commun 2001;282:647-654.
22. Mootha VK, Lindgren CM, Eriksson KF, Subramanian A, Sihag S, Lehar J, et al. PGC-1alpha-responsive genes involved in oxidative phosphorylation are coordinately downregulated in human diabetes. Nat Genet 2003; 34:267-273.
23. Watashi K, Ishii N, Hijikata M, Inoue D, Murata T, Miyanari Y, et al. Cyclophilin B is a functional regulator of hepatitis C virus RNA polymerase. Mol Cell 2005;19:111-122.
24. Nakagawa M, Sakamoto N, Tanabe Y, Koyama T, Itsui Y, Takeda Y, et al. Suppression of hepatitis C virus replication by cyclosporin a is mediated by blockade of cyclophilins. Gastroenterology 2005;129:1031-1041.
25. Lin Y, Nomura T, Cheong J, Dorjsuren D, Iida K, Murakami S. Hepatitis B virus X protein is a transcriptional modulator that communicates with transcription factor IIB and the RNA polymerase II subunit 5. J Biol Chem 1997;272:7132-7139.
26. Moriya K, Fujie H, Shintani Y, Yotsuyanagi H, Tsutsumi T, Ishibashi K, et al. The core protein of hepatitis C virus induces hepatocellular carcinoma in transgenic mice. Nat Med 1998;4:1065-1067.
27. Lerat H, Honda M, Beard MR, Loesch K, Sun J, Yang Y, et al. Steatosis and liver cancer in transgenic mice expressing the structural and nonstructural proteins of hepatitis C virus. Gastroenterology 2002;122:352-365.
28. Adinolfi LE, Gambardella M, Andreana A, Tripodi MF, Utili R, Ruggiero G. Steatosis accelerates the progression of liver damage of chronic hepatitis C patients and correlates with specific HCV genotype and visceral obesity. HEPATOLOGY 2001;33:1358-1364.
29. Monto A, Alonzo J, Watson JJ, Grunfeld C, Wright TL. Steatosis in chronic hepatitis C: relative contributions of obesity, diabetes mellitus, and alcohol. HEPATOLOGY 2002;36:729-736.
30. Raney AK, Kline EF, Tang H, McLachlan A. Transcription and replication of a natural hepatitis B virus nucleocapsid promoter variant is regulated in vivo by peroxisome proliferators. Virology 2001;289:239-251.
31. Guidotti LG, Eggers CM, Raney AK, Chi SY, Peters JM, Gonzalez FJ, et al. In vivo regulation of hepatitis B virus replication by peroxisome proliferators. J Virol 1999;73:10377-10386.
32. Murakami J, Shimizu Y, Kashii Y, Kato T, Minemura M, Okada K, et al. Functional B-cell response in intrahepatic lymphoid follicles in chronic hepatitis C. HEPATOLOGY 1999;30:143-150.
33. Racanelli V, Sansonno D, Piccoli C, D'Amore FP, Tucci FA, Dammacco F. Molecular characterization of B cell clonal expansions in the liver of chronically hepatitis C virus-infected patients. J Immunol 2001;167:21-29.
34. Guleng B, Tateishi K, Ohta M, Kanai F, Jazag A, Ijichi H, et al. Blockade of the stromal cell-derived factor-1/CXCR4 axis attenuates in vivo tumor growth by inhibiting angiogenesis in a vascular endothelial growth factor-independent manner. Cancer Res 2005;65:5864-5871.

ELSEVIER

Journal of Hepatology 44 (2006) 1074–1082

Journal of Hepatology

www.elsevier.com/locate/jhep

A green tea polyphenol, epigalocatechin-3-gallate, induces apoptosis of human hepatocellular carcinoma, possibly through inhibition of Bcl-2 family proteins

T. Nishikawa*, T. Nakajima, M. Moriguchi, M. Jo, S. Sekoguchi, M. Ishii, H. Takashima, T. Katagishi, H. Kimura, M. Minami, Y. Itoh, K. Kagawa, T. Okanoue

Molecular Gastroenterology and Hepatology, Kyoto Prefectural University of Medicine Graduate School of Medical Science, Kawaramachi-Hirokoji, Kamigyo-ku, Kyoto 602-8566, Japan

***Background/Aims*: A major polyphenol of green tea, epigallocatechin-3-gallate (EGCG), has previously been shown to induce cell-cycle arrest and apoptosis in various cancers. However, little is known about its effects on hepatocellular carcinomas (HCCs).**

***Methods*: Four HCC cell lines, HLE, HepG2, HuH-7 and PLC/PRF/5, were treated with EGCG or vehicle. Cell viability was assessed by trypan blue staining and WST-8 assay. Cell-cycle, apoptosis and apoptosis-related proteins in HLE cells were evaluated by flow cytometry and Western blotting. The effect of EGCG was also studied in vivo using a xenograft model. The effect of co-treatment with EGCG and tumor necrosis factor-related apoptosis-inducing ligand (TRAIL) was also assessed.**

***Results*: EGCG inhibited the growth of all HCC cell lines at concentrations of 50–100 μg/ml. In HLE cells, EGCG induced apoptosis but not cell-cycle arrest and appears to have down-regulated Bcl-2α and Bcl-xl by inactivation of NF-κB. Oral administration of EGCG showed similar effects in HLE xenograft tumors. Co-treatment with EGCG and TRAIL synergistically induced apoptosis in HLE cells.**

***Conclusions*: EGCG induced apoptosis in HLE cells, both in vitro and in vivo. Moreover, it enhanced TRAIL-induced apoptosis. Therefore, EGCG treatment may be useful for improving the prognosis of HCCs.**

Keywords: **EGCG; Apoptosis; HCC; NF-κB; Bcl-2 family; TRAIL**

1. Introduction

Epidemiological studies have shown that green tea has anticarcinogenic and anticancer effects [1–5]. A major polyphenol of green tea, epigallocatechin-3-gallate (EGCG), is thought to be the main active ingredient. It is considered to suppress tumor growth indirectly by anti-angiogenic action and activation of immune function [6,7], and directly through cell-cycle arrest and induction of apoptosis mediated by various proteins including p53 and nuclear factor-kappa B (NF-κB) [8,9].

During the progression of hepatocellular carcinoma (HCC), cancer tissues gradually obtain various malignant features in a multistep fashion [10]. Most early-stage HCCs are small tumors with ill-defined boundaries, and consist of well-differentiated cancerous tissues. During the progression, the less differentiated lesions with more malignant properties occasionally arise and replace the preexisting parts. This process increases the malignant potential of a tumor. For this multistep dedifferentiation, HCCs in an advanced stage show poor prognosis, especially when tumors are too large to be treated by surgery or local interventions such as percutaneous ethanol injection therapy (PEIT) and radiofrequency ablation (RFA).

Received 25 July 2005; received in revised form 27 October 2005; accepted 17 November 2005; available online 28 December 2005

* Corresponding author. Tel.: +81 75 251 5519; fax: +81 75 251 0710.
E-mail address: liverresearch2004@yahoo.co.jp (T. Nishikawa).

0168-8278/$32.00
doi:10.1016/j.jhep.2005.11.045

HCCs with poor prognosis are characterized by rapid cell proliferation and strong expression of antiapoptotic genes [11], which suggests that they are mainly due to incomplete cell-cycle arrest and apoptosis-resistance under conventional therapies. To overcome these problems a new or additional therapeutic strategy is needed. In addition, little is known about the anticancer effects and the basic mechanisms of EGCG against HCCs [12,13]. In the present study, we examined the effects of EGCG on growth of human HCC cell lines using an in vitro culture system and an in vivo animal xenograft model, and elucidated the mechanism of growth suppression by analysis of cell-cycle regulation and profiles of proapoptotic and antiapoptotic proteins.

2. Materials and methods

2.1. Cell lines and cell culture

Human HCC cell lines, HLE (an undifferentiated cell line) and HepG2, HuH-7 and PLC/PRF/5 (differentiated cell lines) were purchased from the Health Science Research Resources Bank, Osaka, Japan. Cells were cultured in DMEM supplemented with 10% fetal bovine serum (FBS) and 1% penicillin–streptomycin.

2.2. Antibodies and inhibitors, ligand and EGCG

Antibodies for Bid, Bax, Bcl-2α, Bcl-xl, c-FLIP, AIF, and β-actin were purchased from Lab Vision Corporation (Fremont, CA). Antibodies for survivin, XIAP, cIAP-1/2 and tumor necrosis factor-related apoptosis-inducing ligand (TRAIL) were from R and D Systems Inc. (Minneapolis, MN). An antibody for RIP was from BioVision Research Products (Mountain View, CA). Antibodies for nuclear factor-kappa B (NF-κB) p65 and phospho-NF-κB p65 (Ser536) were from Cell Signaling Technology, Inc. (Beverly, MA). An NF-κB inhibitor, Bay 11-7085 was from Calbiochem (San Francisco, CA). A purified preparation of EGCG (>98% pure) was a kind gift from Dr Yukihiko Hara (Mitsui Norin Ltd, Shizuoka, Japan).

2.3. Cell growth assay

Cells were incubated in 6-well plates (1×10^5 cells/well) for 24 h, then treated with 50 μg/ml EGCG or vehicle. The time of EGCG addition was defined as 0 and cell numbers were counted by trypan blue staining every 24 h (24–96 h). Medium containing the appropriate concentration of EGCG or vehicle was changed every 2 days.

2.4. Cell cytotoxicity assay

Cells were incubated in 96-well plates (5×10^3 cells/well) for 24 h, then treated with EGCG (10, 25, 50 and 100 μg/ml), TRAIL (100 ng/ml) or vehicle. After 24 or 48 h of treatment, the number of viable cells was measured using a WST-8 [2-(2-methoxy-4-nitrophenyl)-3-(4-nitrophenyl)-5-(2,4-disulfophenyl)-2*H*-tetrazolium, monosodium salt] assay (Nacalai Tesque, Kyoto, Japan). Ten microliters WST-8 solution was added into each well and the cells were incubated for another 1 h. The absorbance was measured at a test wavelength of 450 nm and a reference wavelength of 600 nm using a microplate reader (Benchmark, Bio-Rad Laboratories, CA). Cell cytotoxicity was evaluated as the ratio of the absorbance of the sample to that of the control.

2.5. Cell cycle analysis

Cells were incubated for 24 h and then treated with EGCG (10, 25, 50 and 100 μg/ml) or vehicle. Cells (1×10^6) were fixed with 70% ethanol at −20 °C for 24 h, centrifuged, suspended in 1 ml PBS containing RNase A (10 μg/ml), incubated at 37 °C for 30 min, stained with propidium iodide (40 μg/ml), incubated on ice for 30 min and examined with a flow cytometer using Modfit LT software (Becton Dickinson, San Jose, CA).

2.6. Analysis of apoptosis

Cells (5×10^5) that had been treated for 24 h with EGCG (10, 25, 50 and 100 μg/ml), TRAIL (100 ng/ml) or vehicle were labeled with annexin V-FITC and PI using an apoptosis detection kit (BioVision Research Products, Mountain View, CA) according to the manufacturer's protocol. The distribution of apoptotic cells was identified by a flow cytometer using CellQuest software (Becton-Dickinson, San Jose, CA). Cells that were annexin V(−) and PI(−) were considered viable cells. Cells that were annexin V(+) and PI(−) were considered early-stage apoptotic cells. Cells that were annexin V(+) and PI(+) were considered late-stage apoptotic cells or necrotic cells.

2.7. Caspase colorimetric assay

Cytoplasmic protein was extracted from 2×10^6 cells of each cell line that had been treated with EGCG (10, 25, 50 and 100 μg/ml) or vehicle for 24 h. Cytoplasmic protein (150 μg) and 5 μl fluorogenic substrate were added to 50 μl reaction buffer. The mixtures were placed in wells of a 96-well plate and assayed for caspase with a caspase-3, 8, 9 colorimetric assay kit (BioVision Research Products, Mountain View, CA) according to the manufacturer's protocol.

2.8. Western blot

Cells that had been treated with EGCG (10, 25, 50 and 100 μg/ml), Bay 11-7085 (2.0 and 4.0 μg/ml), TRAIL (100 ng/ml) or vehicle for 24 h were lysed using standard procedures. The supernatant was used as cytoplasmic protein. Twenty to fifty micrograms cytoplasmic protein was electrophoresed in a 4–12% bis-tris gel and transferred to a nitrocellulose membrane. The membrane was blocked in 5% nonfat dry milk and incubated with primary antibody for 1 h at room temperature. After incubation with horseradish peroxidase-conjugated secondary antibody for 1 h, antibody-stained bands were detected with SuperSignal West Pico Chemiluminescent Substrate (PIERCE, Rockford, IL). The density of each band was measured using densitography software (ATTO, Tokyo).

2.9. Immunoprecipitation

Cells were treated with 100 μg/ml EGCG for 0, 3, 6, 12 and 24 h. Five hundred microgram of cytoplasmic protein, prepared as described above, was incubated with 60 μl Protein G Sepharose beads (Amersham Biosciences Corp, Piscataway, NJ) for 1 h and centrifuged. The supernatant was incubated with 2 μg *anti*-Bax antibody overnight and with 60 μl Protein G Sepharose beads for another 1 h. The beads were washed 4 times and boiled with 40 μl sample buffer. The immunoprecipitated Bcl-2α and Bcl-xl which bound to Bax were analyzed by Western blot analysis.

2.10. Reverse transcription-polymerase chain reaction (RT-PCR) analysis

Total RNA was extracted from cells that had been treated with EGCG (10, 25, 50 and 100 μg/ml) or vehicle for 24 h and subjected to RT-PCR [14]. Transcripts of the gene for glyceraldehyde-3-phosphate dehydrogenase (G3PDH) were used as an internal control. The primer sequences and amplicon sizes were as follows: bcl-2α forward: 5′-TTGTGGCCTTCTTTGAGTTCG-3′, bcl-2α reverse: 5′-TAC TGCTTTAGTGAACCTTTT-3′ (332 bp product), bcl-xl forward: 5′-GGAGCTGGTGGTTGACTTTCT-3′, bcl-xl reverse: 5′-CCGGAA

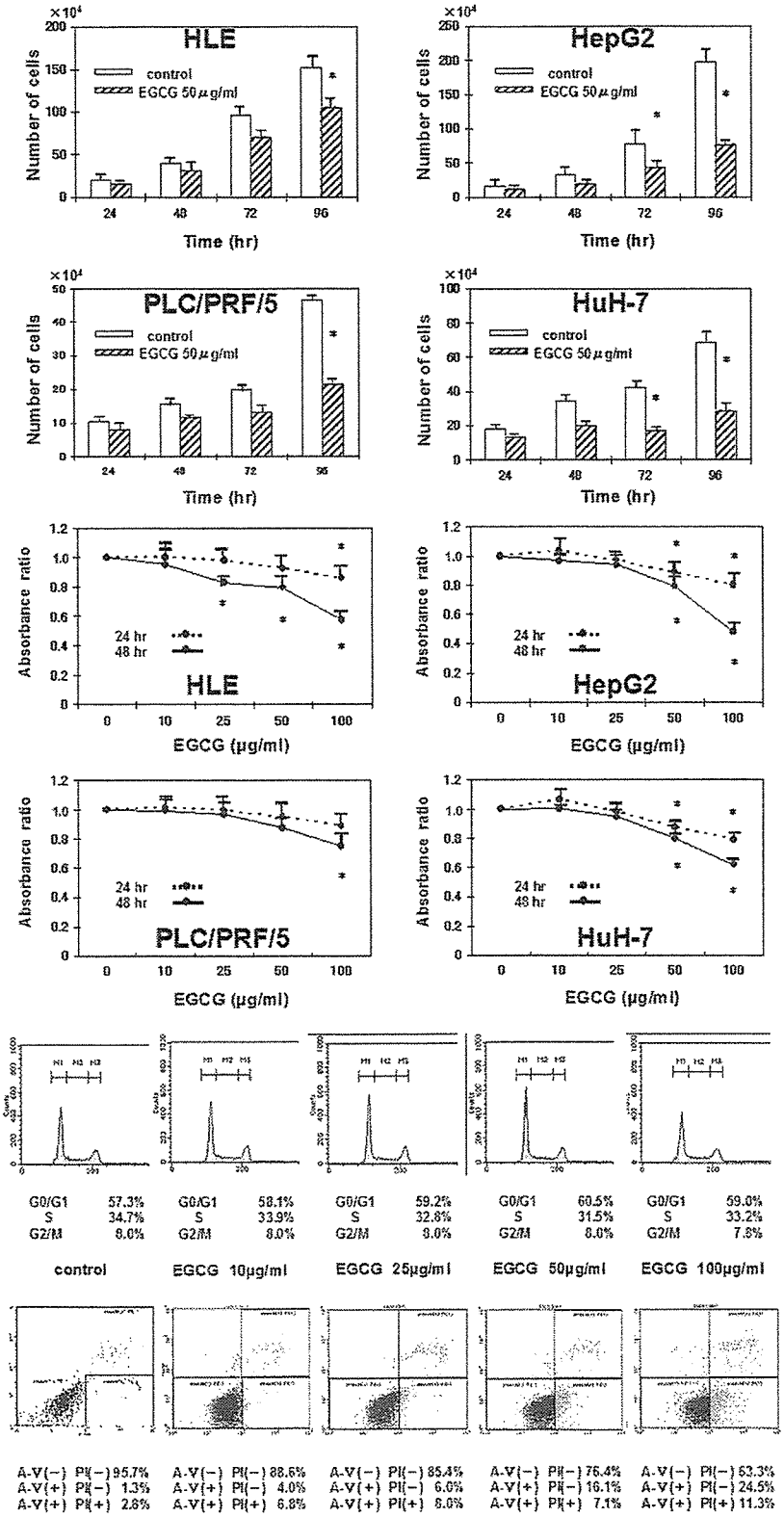

Fig. 1. EGCG inhibits growth of human hepatocellular carcinoma (HCC) cells in vitro and induces apoptosis. (a) Proliferation was assessed in human HCC cell lines, HLE, HepG2, PLC, and HuH-7. The cells were treated with 50 μg/ml EGCG or vehicle for 24, 48, 72 and 96 h, and counted by trypan blue staining. The data represent the mean and SD from five independent experiments. $^{*}P<0.05$. (b) Cell cytotoxicity was assessed using the WST-8

GAGTTCATTCACTAC-3′ (379 bp product), G3PDH forward: 5′-GTCAACGGATTTGGTCGTATT-3′, G3PDH reverse: 5′-AGTCT TCTGGGTGGCAGTGAT- 3′ (540 bp product). The PCR protocol for bcl-2α or bcl-xl consisted of denaturation at 94 °C for 3 min, 32 cycles of denaturation at 94 °C for 30 s, annealing at 55 °C for 30 s and extension at 72 °C for 1 min, final extension at 72 °C for 5 min. The protocol for G3PDH was the same except for annealing at 54 °C for 45 s and amplification for 25 cycles. Amplification was exponential throughout all cycles. The PCR products were electrophoresed in a 1.5% agarose gel and stained with ethidium bromide.

2.11. Growth inhibition of HCC by EGCG in a xenograft model

HLE cells (1×10^6) were injected into the dorsal subcutaneous tissue of twenty 8-week-old nude mice (male BALB/c Slc-nu/nu, Clea Japan, Inc., Tokyo, Japan) to form tumors. Tumor volumes were calculated daily with the formula $(4/3)\pi\{(\text{major axis}/2)\times(\text{minor axis}/2)\}^3$. When the tumor volumes reached 50–250 mm^3, the mice were randomly divided into 4 groups (groups A, B, C, D, $n=5$). The four groups were given sterile water containing 0, 0.8, 2.5 and 7.5 mg/ml EGCG ad libitum, respectively. Water consumption of each group was measured daily. The first day of EGCG water administration was defined as day 0. The mice were weighed every day until day 25 when they were sacrificed. None of the mice in any of the groups showed any obvious changes in body weight, in water consumption or in behavior throughout the experiment. Tumor tissues were collected and fixed in 4% buffered paraformaldehyde. Apoptotic cells were detected with a TUNEL assay and expressions of Bcl-2α and Bcl-xl in HLE cells were assessed with immunohistochemical staining [14]. Animals were treated humanely following the United Kingdom Coordinating Committee on Cancer Research Guidelines.

2.12. Statistical analysis

Differences between groups treated with each concentration of EGCG were assessed using Student's *t*-test. The synergistic effect of EGCG on TRAIL treatment was tested by ANOVA.

3. Results

3.1. EGCG inhibits growth of human HCC cell lines in vitro and induces apoptosis in HLE cells

EGCG treatment inhibited the growth of all of four HCC cell lines in a time-dependent manner (Fig. 1a). The cytotoxicity of EGCG was also observed in all of the cell lines in a dose- and time-dependent manner (Fig. 1b). We selected HLE cells for further investigations because undifferentiated HCC cells such as HLE cells generally show poor prognosis and require a new strategy in clinical practice [15]. EGCG treatment had no effect on cell-cycle progression but induced early-stage apoptosis in a dose-dependent manner (Fig. 1c). The number of cells that were either apoptotic in the delayed stage or necrotic also increased similarly by EGCG treatment. These results suggest that the anti-tumor effect of EGCG in HLE cells is mainly induced by apoptosis.

3.2. EGCG activates caspases and decreases expressions of Bcl-2α and Bcl-xl in HLE cells

EGCG treatment activated caspases-8, 9 and 3 in a dose-dependent manner (Fig. 2a). The caspase-9 pathway is mainly regulated by proteins of the bcl-2 family and inhibitor of apoptosis proteins (IAP) family. The expressions of Bcl-2α and Bcl-xl were gradually inhibited as the EGCG concentration increased. The expressions of Bid and c-IAP2 decreased at higher concentrations of EGCG (50, 100 μg/ml), the former probably due to the cleavage by activated caspase-8. EGCG had no influence on Bax, survivin, XIAP or c-IAP1 (Fig. 2b), c-FLIP and RIP (factors that control the activation of caspase-8), or Fas, the death receptor, or AIF, caspase-independent apoptosis-inducing factor (Fig. 2c). EGCG decreased the bindings of Bcl-2α and Bcl-xl to Bax, which may activate caspase-9 (Fig. 2d).

3.3. EGCG down-regulates the mRNAs of bcl-2α and bcl-xl by inhibition of NF-κB

The mRNA expressions of bcl-2α and bcl-xl decreased following EGCG treatment in a dose-dependent manner (Fig. 3a). Thus, EGCG decreases the expressions of Bcl-2α and Bcl-xl at the level of transcription. EGCG did not affect the protein level of the NF-κB p65 subunit in the cytoplasm but it decreased the active form, phospho-NF-κB p65 (Ser536), (Fig. 3b). When HLE cells were treated with an NF-κB inhibitor, Bay 11-7085 [16], the expressions of Bcl-2α and Bcl-xl decreased in a dose-dependent manner (Fig. 3c). These results appear to show that EGCG down-regulates both Bcl-2α and Bcl-xl expressions via NF-κB inhibition. To examine the time course of these effects, HLE cells were exposed to EGCG for up to 24 h. EGCG treatment inhibited the activation of NF-κB (P65) within 3 h and the effect continued for 24 h (Fig. 3d). The expressions of Bcl-2α and Bcl-xl decreased remarkably after 6 and 3 h of exposure, respectively and continued to decrease, while those of Bax and Fas showed no obvious changes.

3.4. EGCG inhibits growth of HLE in vivo, induces apoptosis and down-regulates Bcl-2α and Bcl-xl

The growth of HLE xenograft tumors in nude mice was suppressed by administration of EGCG compared with the control (Fig. 4a). The inhibitory effect was observed

assay. The cells were treated with EGCG at the indicated concentrations (0—100 μg/ml) and the absorbance ratio was measured in 24 and 48 h. The data represent the mean and SD from ten independent experiments. *$P<0.05$. (c) Effects of EGCG on cell cycle progression and apoptosis in HLE cells were examined by a flow cytometer. The cells were treated as described under Section 2. The proportion of each phase of the cell cycle was analyzed using the Modfit LT software, and apoptosis was assessed using the CellQuest software. The data are from a representative experiment repeated three times with similar results. [This figure appears in colour on the web.]

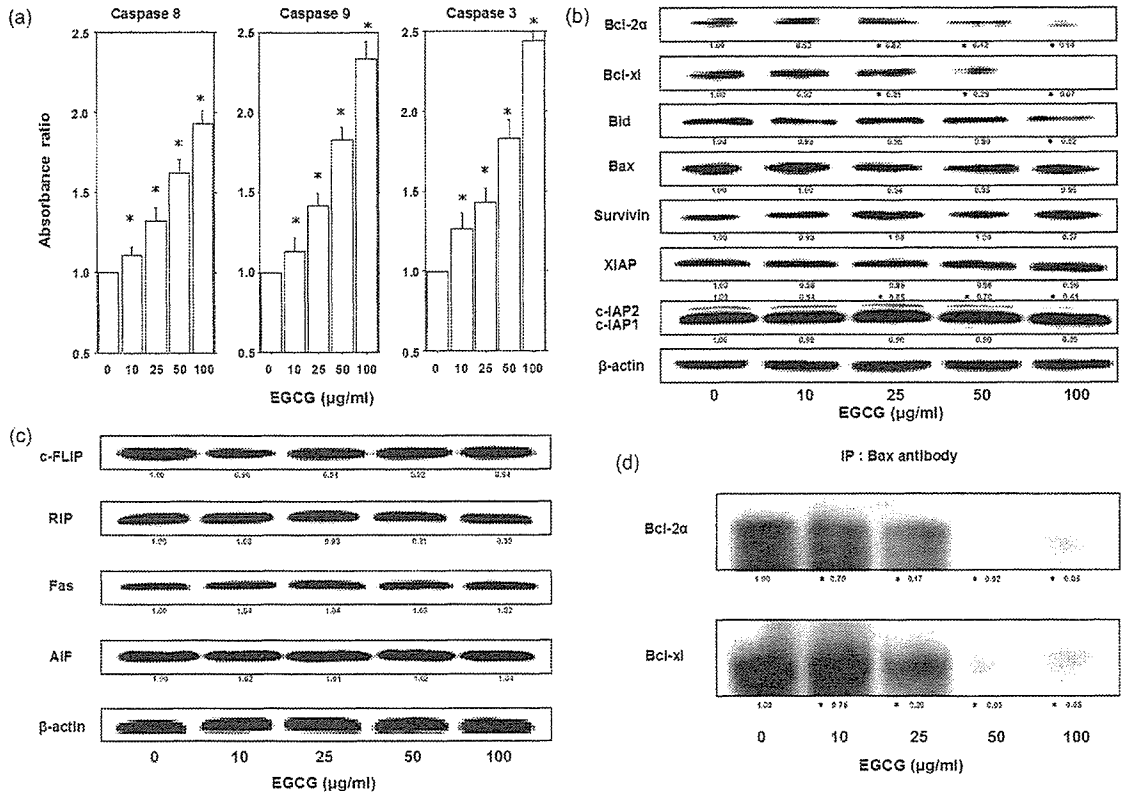

Fig. 2. EGCG activates caspases and decreases expressions of Bcl-2α and Bcl-xl in HLE cells. (a) Activation of caspase-8, -9 and -3 by EGCG in HLE cells. The cells were treated with EGCG at the indicated concentrations (0–100 μg/ml) for 24 h and caspase activities in the cell lysates were measured with a colorimetric assay kit. The data represent the mean and SD from five independent experiments. $^{*}P<0.05$. (b, c) Western blots showing expressions of Bcl-2 family proteins and IAP family proteins (b) and c-FLIP, RIP, Fas and AIF (c) in cells treated with EGCG at the indicated concentrations (0–100 μg/ml) for 24 h. (d) The quantities of Bcl-2α and Bcl-xl binding to Bax were analyzed by immunoprecipitation and Western blot assay. The data shown in each of (b,c) and (d) are representative of three experiments with similar results. Image intensities of a band for a protein p were defined as $(I_p^x/I_c^x)/(I_p^0/I_c^0)$ where I_p^x and I_c^x are the band intensities of the protein and the control (β-actin) at EGCG concentration x and I_p^0 and I_c^0 are the band intensities of the protein and control at EGCG concentration 0. $^{*}P<0.05$.

significantly from day 3 and increased as the concentration of EGCG increased. None of the mice showed any significant difference in body weight, water consumption, or behavior throughout the experiment. The tumor sections showed a large number of apoptotic cells and weak staining of Bcl-2α and Bcl-xl in EGCG-treated mice. In contrast, few apoptotic cells and strong staining of Bcl-2α and Bcl-xl were observed in the control mice (Fig. 4b). These results indicate that oral administration of EGCG induced apoptosis of tumor cells in vivo, probably by down-regulation of Bcl-2α and Bcl-xl.

3.5. EGCG sensitizes HLE cells to TRAIL-mediated apoptosis

HLE cells treated with TRAIL (100 ng/ml) for 24 h showed a weak cytotoxic effect compared with control. However, co-treatment with EGCG and TRAIL significantly enhanced the cytotoxicity in an EGCG dose-dependent manner (Fig. 5a). This effect was significantly different from that of treatment with EGCG alone, and was synergistic ($P<0.0001$ by ANOVA). An apoptosis assay demonstrated similar results (Fig. 5b). EGCG and TRAIL also had a synergistic effect on down-regulating the expressions of Bcl-2α and Bcl-xl in HLE cells (Fig. 5c).

4. Discussion

Advanced HCCs often show poor prognosis even following transcatheter arterial embolization (TAE) or surgical resection [17,18]. Our finding that EGCG inhibited the growth of not only well-differentiated cell lines but also an undifferentiated cell line, HLE (Fig 1a and b) suggests that EGCG has the potential to improve the prognosis of HCCs even in the advanced stage.

Although EGCG can induce apoptosis in various cancers, little is known about its effect on HCC. EGCG was shown to induce cell-cycle arrest and apoptosis through the activation of p53 and Fas-Fas ligand pathways in HepG2 cells [19]. In our experiments, EGCG failed to induce cell-cycle arrest

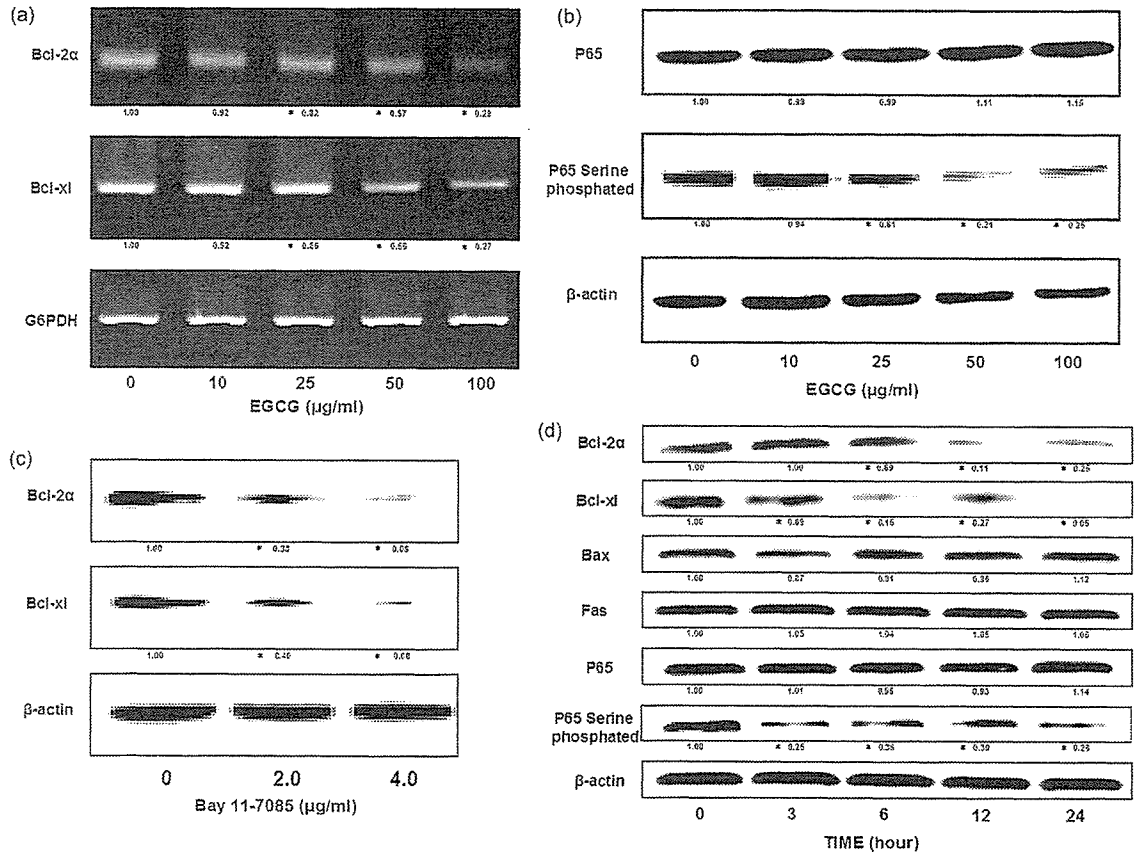

Fig. 3. EGCG inhibits mRNA transcriptions of Bcl-2α and Bcl-xl in HLE cells. (a) Both mRNA expressions of Bcl-2α and Bcl-xl in the cells treated with EGCG at the indicated concentrations (0–100 μg/ml) for 24 h were analyzed by RT-PCR. (b) Activation of NF-κB in the cells was assessed by Western blot assay using antibodies for NF-κB p65 and phospho-NF-κB p65 (Ser536). The cells were treated with EGCG at the indicated concentrations (0–100 μg/ml) for 24 h. (c) Expressions of Bcl-2α and Bcl-xl in the cells treated with the NF-κB inhibitor, Bay 11-7085 at the indicated concentrations (0–4.0 μg/ml) for 24 h. Those expressions were assessed by Western blot assay. (d) Western blot assay showing expressions of Bcl-2α, Bcl-xl, Bax, Fas, NF-κB p65 and phospho-NF-κB p65 (Ser536) in cells treated with 100 μg/ml EGCG for 0, 3, 6, 12 and 24 h. The data shown in each of (a)–(d) are representative of three experiments with similar results. See Fig. 2 for explanation of band intensities. $^{*}P < 0.05$.

but induced apoptosis in HLE cells (Fig. 1c). This is probably because p53 protein in HLE cells is dysfunctional due to a mutation of the p53 gene, whereas it is still functional in HepG2 cells. Additionally, EGCG treatment had no effect on expression of Fas in HLE cells (Figs. 2c and 3d). These results indicate that EGCG has more than one mechanism for inducing apoptosis in HCC. A Western blot assay of pro- and anti-apoptotic proteins showed that EGCG inhibits the expressions of Bcl-2α and Bcl-xl in HLE cells (Fig. 2b), which suggests that activation of caspase-9 by inhibition of Bcl-2α and Bcl-xl is a major mechanism for induction of apoptosis. The inhibition of c-IAP-2 also might contribute to activation of caspase-9. EGCG also activated caspase-8 in HLE cells (Fig. 2a) though it had no effect on the expressions of cFLIP, RIP and Fas (Fig. 2c). The overexpression of Bcl-2 in HCC cells was shown to reduce Fas-mediated apoptosis [20]. EGCG may activate caspase-8 through reactivation of the Fas-Fas ligand pathway by down-regulation of Bcl-2α expression. Another possibility is that EGCG directly activates caspase-8 through its binding to Fas [21].

NF-κB partially regulates the transcriptions of Bcl-2α and Bcl-xl [22]. In addition, our results suggest that EGCG down-regulates the expressions of Bcl-2α and Bcl-xl by inhibition of NF-κB (Fig. 3a–c). NF-κB is a transcriptional factor that is associated with various cellular processes, such as cytokine production, cellular adhesion, cell-cycle activation, apoptotic resistance, oncogenesis, and is activated in various solid tumors [23]. Thus, the inhibitory effect of EGCG on NF-κB may suppress the growth of various cancer cells in multifunctional ways. NF-κB activation is induced by reactive oxygen species [24] and inhibited by antioxidants [25]. Thus, the inhibitory effect of EGCG on NF-κB activation may be due to its strong ability to scavenge reactive oxygen species. Bcl-xl overexpression is frequently found in HCC tissues and is significantly correlated with a good prognosis [26,27]. On the other hand, Bcl-2α is not frequently expressed in HCCs [28], but TAE

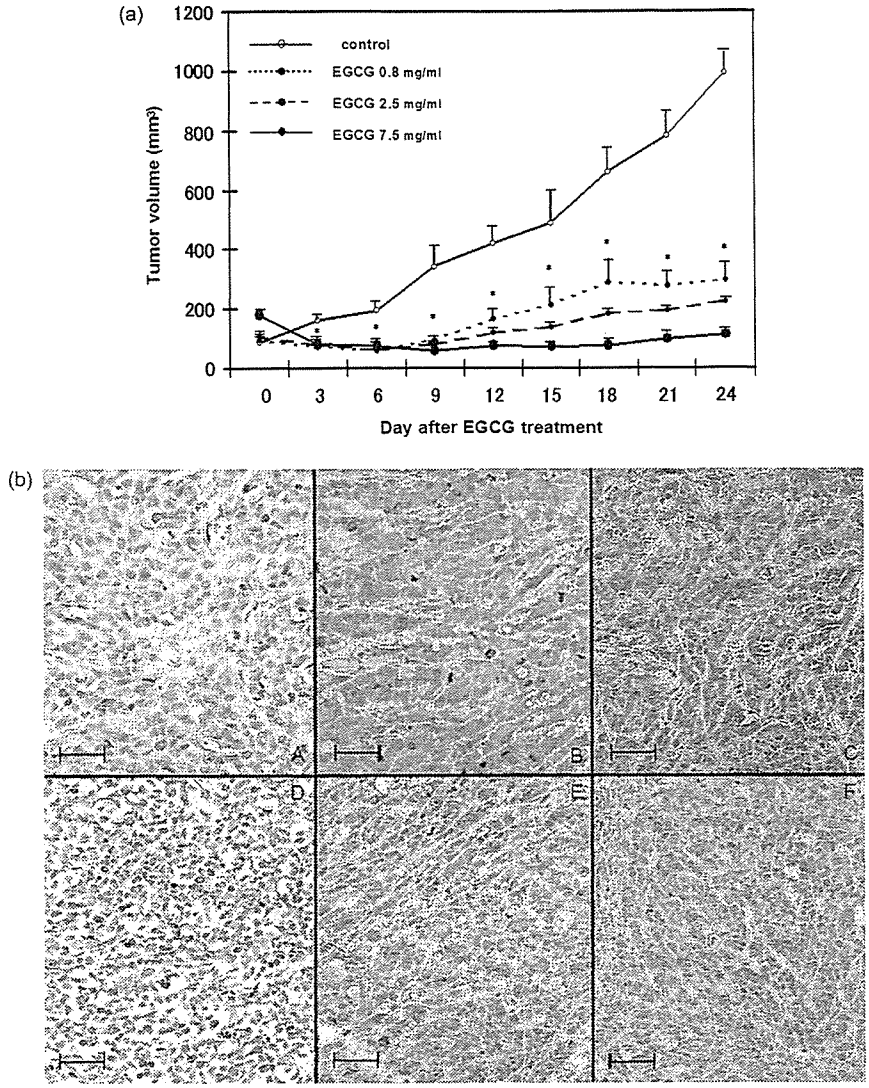

Fig. 4. (a) Growth curve of HLE xenografts in nude mice. Nude mice were injected with approximately 1×10^6 HLE cells into the dorsal subcutaneous tissue. When the tumor volumes reached 50–250 mm^3, the mice were divided into four groups and fed with sterile water or 0.8, 2.5, 7.5 mg/ml EGCG water respectively. The data represent the mean and SD from five nude mice. $^*P < 0.05$. (b) Apoptosis and expressions of Bcl-2α and Bcl-xl in HLE xenografts. Apoptosis was assessed by TUNEL assay (A, D) and expressions of Bcl-2α (B, E) and Bcl-xl (C, F) were assessed by immunohistochemistry. The upper row shows tumor sections in the control group and the lower row shows tumor sections in the group receiving 7.5 mg/ml EGCG. Each picture was taken at a magnification of 400×. Scale bars, 50 μm.

increases its expression in HCC tissues [29]. The induction of Bcl-2α by TAE may allow the cancer cells to escape from hypoxic injury. Furthermore, these antiapoptotic proteins are associated with resistance to chemotherapy [30] and to endogenous apoptotic signals such as TRAIL [31,32] both in vitro and in vivo. In our experiment, EGCG treatment down-regulated both Bcl-2α and Bcl-xl in HLE cells (Figs. 2b and 4b) both in vitro and in vivo and sensitized HLE cells to TRAIL-induced apoptosis in vitro (Fig. 5a and b). The sensitizing effect of EGCG appears to result from the down-regulation of Bcl-2α and Bcl-xl through inhibition of NF-κB (Fig. 5c).

Our findings that EGCG suppresses the growth of HLE cells (Fig. 4a) and down-regulates the expressions of Bcl-2α and Bcl-xl in vivo (Fig. 4b) raise the possibility that oral administration of EGCG can help overcome the chemotherapy resistance of HCCs. However, the concentrations of EGCG that were needed to significantly down-regulate *anti*-apoptotic proteins and induce apoptosis in vitro (50–100 μg/ml) were much higher than the concentration that is physiologically achieved by ordinary green tea consumption. Consumption of six or seven cups of green tea per day (corresponding to a dose of ~30 mg EGCG/kg per day) will result in a plasma EGCG concentration of approximately 1 μg/ml [33]. However,

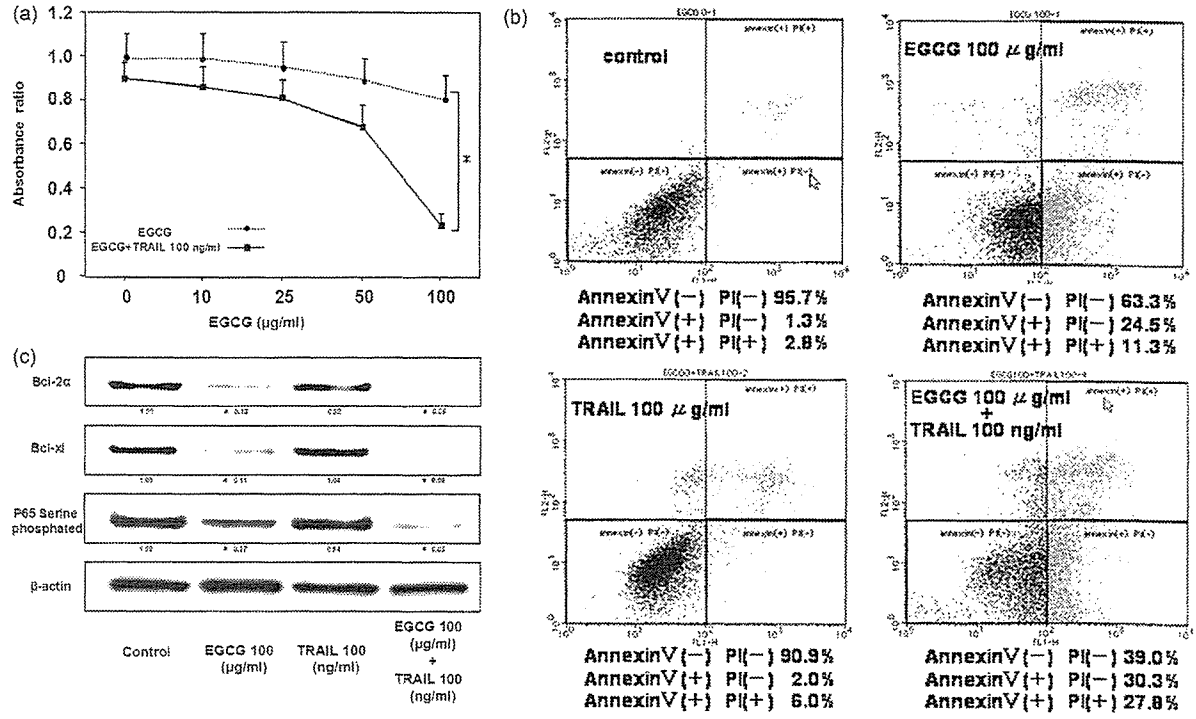

Fig. 5. EGCG sensitizes HLE cells to TRAIL-mediated apoptosis. (a) Cell cytotoxicity was assessed using the WST-8 assay in the cells treated with vehicle or 100 μg/ml EGCG or 100 ng/ml TRAIL or combinations of these agents for 24 h. The combination treatment significantly enhanced the cell cytotoxicity compared with EGCG treatment alone. The data represent the mean and SD from five independent experiments. $^{*}P<0.0001$ by ANOVA. (b) Apoptosis in the cells treated as described above was examined by flow cytometry. The experiment was repeated three times with similar results. (c) Western blot assay showing expressions of Bcl-2α, Bcl-xl and phospho-NF-κB p65 (Ser536) in cells treated with vehicle or 100 μg/ml EGCG or 100 ng/ml TRAIL or combinations of these agents for 24 h. The data shown in (c) is representative of three experiments with similar results. See Fig. 2 for explanation of band intensities. $^{*}P<0.05$. [This figure appears in colour on the web.]

higher plasma EGCG concentrations can be achieved by taking EGCG supplements [34]. In our study, EGCG had no obvious adverse effects on the growth or behavior of mice, even at a dose of 1125 mg/kg per day. EGCG also has an antiangiogenic effect and activates an immune response against tumors, which may increase its antitumor effect in vivo.

In conclusion, our results show that EGCG treatment inhibited the growth of HLE cells in vitro and in vivo. The inhibition was caused by the induction of apoptosis as a result of the activations of caspase-8, -9 and -3. These caspases appear to be activated by the down-regulation of Bcl-2α and Bcl-xl through inhibition of NF-κB. Our results indicate that EGCG treatment may be useful in clinical cases to improve the prognosis of advanced HCCs by direct induction of apoptosis and by enhancing the effects of other factors such as TRAIL.

Acknowledgements

We thank Dr Yukihiko Hara for providing the purified preparation of EGCG. We thank an anonymous reviewer for many helpful suggestions.

References

[1] Nakachi K, Matsuyama S, Miyake S, Suganuma M, Imai K. Preventive effects of drinking green tea on cancer and cardiovascular disease: epidemiological evidence for multiple targeting prevention. Biofactors 2000;13:49–54.

[2] Imai K, Suga K, Nakachi K. Cancer-preventive effects of drinking green tea among a Japanese population. Prev Med 1997;26:769–775.

[3] Hibasami H, Komiya T, Achiwa Y, Ohnishi K, Kojima T, Nakanishi K, et al. Induction of apoptosis in human stomach cancer cells by green tea catechins. Oncol Rep 1998;5:527–529.

[4] Sartippour MR, Heber D, Ma J, Lu Q, Go VL, Nguyen M. Green tea and its catechins inhibit breast cancer xenografts. Nutr Cancer 2001; 40:149–156.

[5] Berger SJ, Gupta S, Belfi CA, Gosky DM, Mukhtar H. Green tea constituent (−)-epigallocatechin-3-gallate inhibits topoisomerase I activity in human colon carcinoma cells. Biochem Biophys Res Commun 2001;288:101–105.

[6] Jung YD, Ellis LM. Inhibition of tumour invasion and angiogenesis by epigallocatechin gallate (EGCG), a major component of green tea. Int J Exp Pathol 2001;82:309–316.

[7] Zhu M, Gong Y, Yang Z, Ge G, Han C, Chen J. Green tea and its major components ameliorate immune dysfunction in mice bearing lewis lung carcinoma and treated with the carcinogen NNK. Nutr Cancer 1999;35:64–72.

[8] Gupta S, Hussain T, Mukhtar H. Molecular pathway for (−)-epigallocatechin-3-gallate-induced cell cycle arrest and apoptosis of human prostate carcinoma cells. Arch Biochem Biophys 2003;410: 177–185.

[9] Hastak K, Gupta S, Ahmad N, Agarwal MK, Agarwal ML, Mukhtar H. Role of p53 and NF-kappaB in epigallocatechin-3-gallate-induced apoptosis of LNCaP cells. Oncogene 2003;22: 4851–4859.
[10] Kenmochi K, Sugihara S, Kojiro M. Relationship of histologic grade of hepatocellular carcinoma (HCC) to tumor size, and demonstration of tumor cells of multiple different grades in single small HCC. Liver 1987;7:18–26.
[11] Lee JS, Chu IS, Heo J, Calvisi DF, Sun Z, Roskams T, et al. Classification and prediction of survival in hepatocellular carcinoma by gene expression profiling. Hepatology 2004;40:667–676.
[12] Wei DZ, Yang JY, Liu JW, Tong WY. Inhibition of liver cancer cell proliferation and migration by a combination of (−)-epigallocatechin-3-gallate and ascorbic acid. J Chemother 2003;15:591–595.
[13] Uesato S, Kitagawa Y, Kamishimoto M, Kumagai A, Hori H, Nagasawa H. Inhibition of green tea catechins against the growth of cancerous human colon and hepatic epithelial cells. Cancer Lett 2001; 170:41–44.
[14] Moriguchi M, Nakajima T, Kimura H, Watanabe T, Takashima H, Mitsumoto Y, et al. The copper chelator trientine has an antiangiogenic effect against hepatocellular carcinoma, possibly through inhibition of interleukin-8 production. Int J Cancer 2002; 102:445–452.
[15] Tarao K, Shimizu A, Harada M, Ohkawa S, Okamoto N, Kuni Y, et al. In vitro uptake of bromodeoxyuridine by human hepatocellular carcinoma and its relation to histopathologic findings and biologic behavior. Cancer 1991;68:1789–1794.
[16] Pierce JW, Schoenleber R, Jesmok G, Best J, Moore SA, Collins T, et al. Novel inhibitors of cytokine-induced IkappaBalpha phosphorylation and endothelial cell adhesion molecule expression show anti-inflammatory effects in vivo. J Biol Chem 1997;272:21096–21103.
[17] Wang Y, Zhang J, Gao Y, Yu M, Gong Y, Yu G. Therapeutic efficacy of transcatheter arterial embolization of primary hepatocellular carcinoma: discrepancy in different histopathologic subtypes. Chin Med J Engl 1999;112:264–268.
[18] Ariizumi S, Takasaki K, Yamamoto M, Ohtsubo T, Katsuragawa H, Katagiri S. Histopathologic differentiation of the main nodule determines outcome after hepatic resection for synchronous multicentric hepatocellular carcinomas. Hepatogastroenterology 2004;51: 500–504.
[19] Kuo PL, Lin CC. Green tea constituent (−)-epigallocatechin-3-gallate inhibits Hep G2 cell proliferation and induces apoptosis through p53-dependent and Fas-mediated pathways. J Biomed Sci 2003;10:219–227.
[20] Takahashi M, Saito H, Okuyama T, Miyashita T, Kosuga M, Sumisa F, et al. Overexpression of Bcl-2 protects human hepatoma cells from Fas-antibody-mediated apoptosis. J Hepatol 1999;31: 315–322.
[21] Hayakawa S, Saeki K, Sazuka M, Suzuki Y, Shoji Y, Ohta T, et al. Apoptosis induction by epigallocatechin gallate involves its binding to Fas. Biochem Biophys Res Commun 2001;285:1102–1106.
[22] Tamatani M, Che YH, Matsuzaki H, Ogawa S, Okado H, Miyake S, et al. Tumor necrosis factor induces Bcl-2 and Bcl-x expression through NFkappaB activation in primary hippocampal neurons. J Biol Chem 1999;274:8531–8538.
[23] Schwartz SA, Hernandez A, Mark Evers B. The role of NF-kappaB/IkappaB proteins in cancer: implications for novel treatment strategies. Surg Oncol 1999;8:143–153.
[24] Hughes G, Murphy MP, Ledgerwood EC. Mitochondrial reactive oxygen species regulate the temporal activation of nuclear factor kappa B to modulate tumour necrosis factor-induced apoptosis: evidence from mitochondria-targeted antioxidants. Biochem J 2005; 23 [Epub ahead of print].
[25] Suzuki YJ, Packer L. Inhibition of NF-kappa B activation by vitamin E derivatives. Biochem Biophys Res Commun 1993;193:277–283.
[26] Takehara T, Liu X, Fujimoto J, Friedman SL, Takahashi H. Expression and role of Bcl-xL in human hepatocellular carcinomas. Hepatology 2001;34:55–61.
[27] Watanabe J, Kushihata F, Honda K, Sugita A, Tateishi N, Mominoki K, et al. Prognostic significance of Bcl-xL in human hepatocellular carcinoma. Surgery 2004;135:604–612.
[28] Charlotte F, L'Hermine A, Martin N, Geleyn Y, Nollet M, Gaulard P, et al. Immunohistochemical detection of bcl-2 protein in normal and pathological human liver. Am J Pathol 1994;144:460–465.
[29] Kobayashi N, Ishii M, Ueno Y, Kisara N, Chida N, Iwasaki T, et al. Co-expression of Bcl-2 protein and vascular endothelial growth factor in hepatocellular carcinomas treated by chemoembolization. Liver 1999;19:25–31.
[30] Chun E, Lee KY. Bcl-2 and Bcl-xL are important for the induction of paclitaxel resistance in human hepatocellular carcinoma cells. Biochem Biophys Res Commun 2004;315:771–779.
[31] Kim IK, Jung YK, Noh DY, Song YS, Choi CH, Oh BH, et al. Functional screening of genes suppressing TRAIL-induced apoptosis: distinct inhibitory activities of Bcl-XL and Bcl-2. Br J Cancer 2003; 88:910–917.
[32] Guo BC, Xu YH. Anti-human hepatocellular carcinoma effects of tumor necrosis factor-related apoptosis-inducing ligand in vitro & in vivo. Acta Pharmacol Sin 2001;22:831–836.
[33] Yang CS, Chen L, Lee MJ, Balentine D, Kuo MC, Schantz SP. Blood and urine levels of tea catechins after ingestion of different amounts of green tea by human volunteers. Cancer Epidemiol Biomarkers Prev 1998;7:351–354.
[34] Chow HH, Cai Y, Alberts DS, Hakim I, Dorr R, Shahi F, et al. Phase I pharmacokinetic study of tea polyphenols following single-dose administration of epigallocatechin gallate and polyphenon E. Cancer Epidemiol Biomarkers Prev 2001;10:53–58.

ELSEVIER

Journal of Hepatology 45 (2006) 681–687

Journal of Hepatology

www.elsevier.com/locate/jhep

In vivo selection of transduced hematopoietic stem cells and little evidence of their conversion into hepatocytes in vivo☆

Kanji Yamaguchi[1,2], Katsuhiko Itoh[1,*], Tomoko Masuda[1], Atsushi Umemura[1], Christopher Baum[3], Yoshito Itoh[2], Takeshi Okanoue[2], Jun Fujita[1]

[1]*Department of Clinical Molecular Biology, Faculty of Medicine, Kyoto University, Kyoto, Japan*
[2]*Molecular Gastroenterology and Hepatology, Kyoto Prefectural University of Medicine, Graduate School of Medicine, Kyoto, Japan*
[3]*Department of Hematology/Oncology, Hannover Medical School, Hannover, Germany*

Background/Aims: **FMEV-type retroviral vector provides high transgene expression in hepatocytes and hematopoietic stem cells (HSCs). Here, we examined whether these vectors could provide a sufficient drug-resistance gene expression in HSCs and whether transduced HSCs could differentiate into hepatocytes in vivo.**

Methods: **The $CD45^+/Lin^-$ cells were transduced in vitro by FMEV-type vectors containing human O^6-methylguanine–DNA methyltransferase (MGMT)/reporter genes and transferred into recipient mice. After the treatment with temozolomide and O^6-benzylguanine (TMZ/BG) in vivo, we analyzed the transgene expression in peripheral blood cells by flow-cytometry. Immunohistochemistry was performed on the liver slices in partial hepatectomized recipient mice.**

Results: **After TMZ/BG treatment, transduced host cells were enriched in recipient mice. In the liver, we observed the efficient transgene expression in many small cells along sinusoids. However, only few large cells in hepatic lobules expressed albumin. They also expressed both a transgene and a recipient marker gene, suggesting the fusion of donor HSCs with recipient hepatocytes.**

Conclusions: **This vector expressed a drug-resistance gene in HSCs highly enough to protect them from the drugs. But, the conversion of HSCs into hepatocytes in vivo might be a rare event in this model.**

Keywords: **FMEV-type retroviral vector; Hematopoietic stem cell; In vivo selection; Transdifferentiation; Hepatocytes**

1. Introduction

Retroviral vectors are the most commonly used gene transfer vehicles for various cell types [1] and the liver is one of the attractive targets for gene therapy, since it synthesizes pivotal proteins for metabolism or hemostasis [2]. We have already reported that a FMEV-type retroviral vector containing the polycythemic strain of spleen focus-forming virus (SFFVp) long terminal repeats (LTR) and the mouse embryonic stem cell virus (MESV) leader sequences efficiently express transgenes in HSCs [3–5] as well as hepatocytes [6,7].

The human O^6-methylguanine–DNA methyltransferase (MGMT) gene is one of the multidrug resistance (MDR) genes. The MGMT protein removes alkyl adducts from the O^6 position of guanine before the

Received 22 December 2005; received in revised form 29 March 2006; accepted 14 April 2006; available online 30 May 2006

☆ The authors who have taken part in the research of this paper have no relationship with the manufacturers of the drug involved either in the past or present. The authors state that they did not receive funding from the manufacturers to carry out their research. The authors received funding from Grants-in-Aid from the Ministry of Education, Science, Sports and Culture of Japan which enabled them to carry out their study.

* Corresponding author. Tel.: +81 75 751 3753; fax: +81 75 751 3750.

E-mail address: katsu@virus.kyoto-u.ac.jp (K. Itoh).

Abbreviations: HSC, hematopoietic stem cell; MGMT, O^6-methylguanine–DNA methyltransferase; TMZ, temozolomide; BG, O^6-benzylguanine; MDR, multidrug resistance; GFP, green fluorescein protein; PBNC, peripheral blood nucleated cell; Wt, wild-type.

0168-8278/$32.00
doi:10.1016/j.jhep.2006.04.012

drug-induced reaction that leads to irreversible cell death. Most of tumor cells can resist alkylating agents, such as nitrosoureas, through increased wild-type MGMT expression. But this resistance is inhibited by the treatment with O^6-benzylguanine (BG), which acts by inactivating wild-type MGMT. P140K [8] gene is one of the BG-resistant MGMT variants. Retroviral vectors carrying these MDR genes are used for the protection of hematopoietic stem cells (HSCs) from anticancer drugs [9].

In the treatment of liver primary and metastatic tumors, intensive chemotherapy cannot be performed because a pancytopenia or severe liver failure is frequently seen in the patient of the decompensated liver cirrhosis stage. Transfer of a MDR gene into HSCs would enable to protect cancer patient from drug-induced myelosuppression. Furthermore several studies have demonstrated that bone marrow-derived adult stem cells are capable of transdifferentiation into multiple organs, including the liver [10,11]. This indicates the possibility that the transfer of a MDR gene into HSCs would enable the protection from not only myelosuppression but also the liver damage.

In the present report, we have examined whether the vectors express a MGMT gene in HSCs highly enough to protect them from TMZ/BG combined therapy in vivo. We also examined whether the transduced HSCs could transdifferentiate into hepatocytes and whether the transdifferentiate hepatocytes express the transgene in vivo.

2. Materials and methods

2.1. Reagents and antibodies

BG was purchased from Sigma and TMZ was provided from Shering-Plough Research Institute (Kenilworth, NJ). Recombinant murine stem cell factor, thrombopoietin and Flt-3 ligand were purchased from Chemicon International, R&D Systems and Genzyme/Techne, respectively.

Anti-mouse monoclonal antibodies (MoAbs) of peridinin chlorophyll *a* protein cyanine 5.5-OSu-conjugated CD45 (PerCPCy5.5-CD45, 30-F11), phycoerythrin-conjugated Thy-1 (PE-Thy-1, G7), biotinylated B220 (B-B220, RA3-6B2) and Gr-1 (B-Gr-1, RB6-8C5) were purchased from BD Biosciences, streptavidin-PC5 (st.-PC5) from Coulter Japan. A MoAb of anti-mouse c-kit (ACK2) was purified from hybridoma culture supernatant and conjugated with fluorescein isothiocyanate (FITC-c-kit). These were used for the study using a fluorescein-activated cell sorter or flow-cytometric analysis.

MoAbs of anti-human MGMT (MT3.1), anti-actin (C4), biotinylated anti-F4/80 (BM8), anti-green fluorescein protein (GFP, GFP-20) or PE-conjugated anti-mouse IgG kappa were purchased from Kamiya Biomedical, Chemicon International, Acris Antibodies, Sigma or Cell Lab, respectively, and a goat anti-luciferase, anti-CD68 (sc-5474) or FITC-conjugated anti-albumin antibodies from Promega Japan, Santa Cruz or Berhyl lab, respectively. A horseradish peroxidase (HRP)-conjugated goat anti-mouse IgG, a F(ab')2 fragment of a FITC-conjugated goat anti-mouse IgG(H+L), streptavidin-FITC (st.-FITC) and FITC-, PE- or Alexa647-conjugated anti-goat IgG(H+L) antibodies were from Dako Japan, Immunotech, Coulter Japan, Caltag, IMGENEX or InVitrogen, respectively. These were used for the studies of immunoblotting and immunohistochemistry.

2.2. Plasmids

Based on a vector plasmid, pSF1N/CMV [12], we have constructed retroviral vector plasmids, pSF-GFP/MGMT and pSF-luc/MGMT, by ligating a *NotI–HindIII* fragment containing a reporter gene, GFP, internal ribosome entry site (IRES) of NF-κB repressing factor [13] and a variant of human MGMT (P140K) or a luciferase gene into a vector plasmid, pSF1N/CMV, respectively.

2.3. Mice

We purchased 8–10-week-old C57BL/6 mice from Shimizu Experimental Animal Farm (Shizuoka, Japan) and GFP transgenic mice (GFP-Tg mice), TgN(β-act-EGFP)Osb [14], were kindly provided by Dr. M. Okabe of Osaka University.

We hepatectomized mice (70% partial hepatectomy) 3 weeks before immunohistochemical analysis of the liver.

2.4. Cells

A human hematopoietic cell line, K562, and an amphotropic retrovirus packaging cell line, Phoenix-ampho [15], were maintained in DMEM supplemented with 10% fetal calf serum and an ecotropic retrovirus packaging cell line, GP+E86 [16], with 10% calf serum. A murine stromal cell line, MS-5 [17], was maintained in alpha-medium with 20% horse serum.

We established etroviral vector producing clones by transfecting plasmids of pSF-GFP/MGMT or pSF-luc/MGMT into GP+E86 cells followed by limited dilution.

2.5. Transduction and transplantation of cells

After transfecting pSF-GFP/MGMT into Phoenix-ampho cells, we used the supernatant containing viral vectors to transduce K562 cells.

After depleting hematopoietic differentiation marker-positive bone marrow cells using SpinSep (Stem Cell Technologies), we stained these cells (Lin^-) with FITC-c-kit and PerCPCy5.5-CD45, followed by separation of CD45-positive cells (Fig. 2B, region "A") using a fluorescein-activated cell sorter, Epics Elite (Coulter Japan). We transduced these sorted cells ($Lin^-/CD45^+$) using essentially the same protocol as previously described [5]. In brief, we overlaid cells on top of mixed culture of irradiated virus producing clones of GP+E86 cells and MS-5 and cultured them in the presence of stem cell factor (50 ng/ml), thrombopoietin (25 ng/ml) and Flt-3 ligand (200 ng/ml) for 10 days. We transplanted 2×10^4 these transduced cells into a 850 cGy-irradiated recipient mouse via tail vain.

2.6. Enrichment of transduced cells with TMZ and BG

Transduced K562 were exposed to 40 μM BG for 1 h, followed by culture in the presence of 100 μM or 400 μM TMZ for 2.5 h. After washing, we additionally exposed cells to BG for 12 h and evaluated the proportion of cells expressing GFP on a flow-cytometer (Epics XL, Coulter Japan) after 7 days of culture.

Nine weeks after transplantation, mice were treated twice with TMZ and BG intraperitoneally (0.6 mg of TMZ and 1 mg of BG per mouse per day) for 5 days, in each of treatment courses separated by a 4-week interval as schematically shown in Fig. 3. We stained peripheral blood nucleated cells (PBNCs) with PE-Thy-1 or B-B220, B-Gr-1, followed by st.-PC5, and evaluated the proportion of cells expressing GFP.

2.7. Immunoblotting

Immunoblotting was performed as previously described [18] using anti-MGMT, anti-luciferase or anti-actin antibodies and a HRP-conjugated secondary antibody.

2.8. Immunohistochemical analysis

Immunohistochemical analysis was performed as previously described [18] using anti-GFP, anti-F4/80, anti-CD68, anti-luciferase, anti-MGMT or anti-albumin antibodies and FITC- or PE-conjugated secondary antibodies or a secondary reagent, st.-FITC.

3. Results

3.1. Enrichment of transduced hematopoietic K562 cells in vitro

We constructed a series of retroviral vectors containing the SFFVp LTR and the MESV leader sequences. These vectors carry a variant gene of human methylguanine methyltransferase, P140K [8], at the downstream position of IRES. First, one of these vectors, SF-GFP/MGMT (Fig. 1A), was examined in vitro whether the transduced cells can be protected from the combination of BG, a drug which depletes wild-type cells of MGMT activity, and TMZ, a DNA-methylating drug. Human hematopoietic K562 cells were transduced by SF-GFP/MGMT and exposed to the combination of these drugs (BG/TMZ). Proportions of cells expressing a GFP gene were small without transduction or without selection (0.2% or 4.2%, respectively), while the cells expressing GFP were efficiently selected by the exposure to BG/TMZ in a dose-dependent manner (Fig. 1A). To confirm the efficient expression of transgenes by the vector, we did Western blotting. Expression of MGMT was undetectable in cells untransduced or unexposed to BG/TMZ, while clear bands were detected in cells after the selection by BG/TMZ (Fig. 1B). These results indicated that transgenes were efficiently expressed by using the vector.

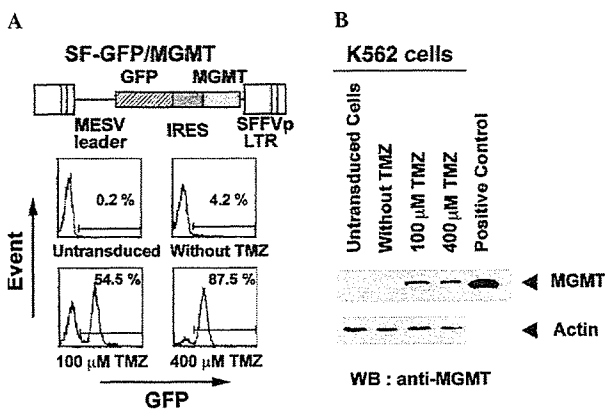

Fig. 1. In vitro selection of transduced cells. (A) Selection of transduced K562 cells in vitro. We evaluated the proportion of transduced K562 cells expressing GFP using a flow-cytometer after 7 days of culture. (B) A human MGMT protein in K562 cells was detected by Western blotting after in vitro selection.

3.2. Enrichment of transduced HSCs in vivo

To examine whether these vectors protect HSCs from the exposure of BG/TMZ in vivo, $Lin^-/CD45^+$ cells from bone marrow cells of GFP-Tg mice or wild-type (Wt) were sorted (Fig. 2B, region A). We transduced these sorted cells with the vectors, SF-luc/MGMT and SF-GFP/MGMT, carrying MGMT and a luciferase gene or a GFP gene, respectively (Fig. 2A), and transferred into sub-lethally irradiated (850 cGy) recipient mice (Fig. 2A). After transplantation, we treated mice twice with TMZ/BG as schematically shown in Fig. 2C.

Fig. 3A shows the number of nucleated cells in peripheral blood (PBNCs) during the treatment. Although the number of PBNCs was drastically decreased after the first treatment with BG/TMZ, the number was not changed significantly after the second treatment (Fig. 3A), suggesting that gene-modified HSCs were enriched by the first treatment and HSCs were protected from the second treatment.

To examine the proportion of retrovirally transduced cells during the treatment, we transduced $Lin^-/CD45^+$ cells of Wt mice with SF-GFP/MGMT vector and transferred into irradiated Wt mice (Fig. 2A, Wt > Wt). Flow-cytometric analysis showed that proportion of GFP-positive (GFP+) cells in PBNCs was 8.8% before the treatment and increased to 20.4% and 74.1% after the first and second treatment, respectively (Fig. 3B). Next, we examined the proportion of donor-derived cells in PBNCs. Fig. 3C shows the proportion of GFP+ cells in B220-positive (B cells), Thy-1-positive (T cells) and Gr-1-positive (granulocytes) populations during the treatment. When we transferred transduced $Lin^-/CD45^+$ cells from a GFP-Tg mouse into Wt mice (GFP > Wt), proportion of GFP+ cells in B, T cells and granulocytes increased after the BG/TMZ treatment. While the proportion in these cells decreased when we transferred the cells from a Wt mouse into GFP-Tg mice (Wt > GFP), indicating successful enrichment of transduced donor HSCs in vivo. Results of Western blotting of PBNCs in Wt > GFP mice demonstrated that PBNCs expressed detectable amount of luciferase (Fig. 3D) or MGMT (Fig. 3E) after the treatment, confirming the enrichment of transduced cells in vivo. All of these data indicate that FMEV-type vectors express a drug-resistance gene in HSCs highly enough to protect them from the treatment of drugs in vivo.

3.3. Little evidence of transdifferentiation of $Lin^-/CD45^+$ hematopoietic cells into hepatocytes in vivo

We examined the expression of transgenes in the liver of recipient mice seven days after partial hepatectomy and found GFP+ cells in the wall of blood vessels and along sinusoid in the liver lobules of Wt > Wt mice (Fig. 4A, lower column) and GFP > Wt mice

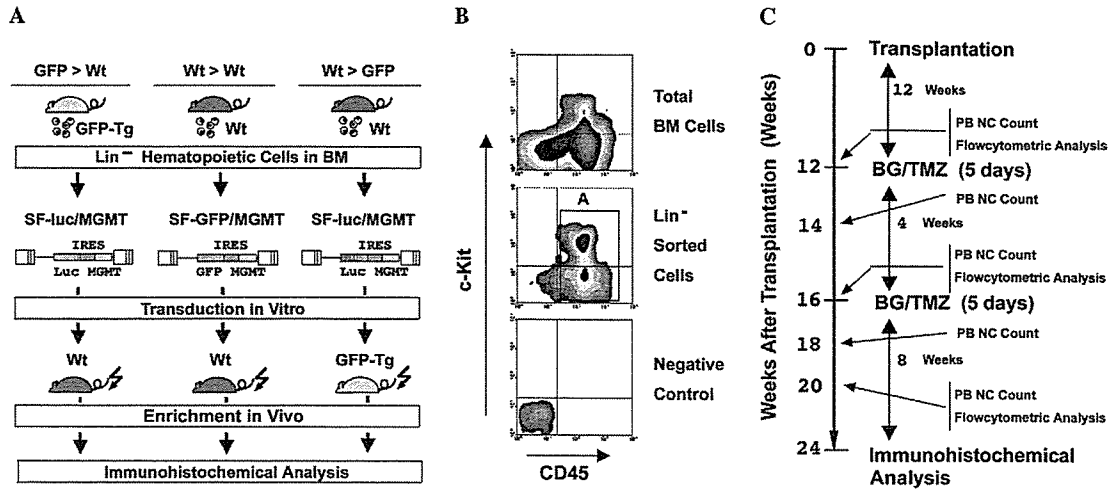

Fig. 2. (A) Schematic illustration of the experimental design. We used $Lin^-/CD45^+$ cells of GFP-Tg mice or wild-type mice as a source of donor HSCs for irradiated Wt recipients (GFP > Wt or Wt > Wt, respectively), or $Lin^-/CD45^+$ cells of Wt for GFP-Tg (Wt > GFP). We transduced these cells by retroviral vectors, SF-luc/MGMT and SF-GFP/MGMT, and transferred into recipient mice via tail vein. (B) Enrichment of $Lin^-/CD45^+$ hematopoietic cells. After enrichment of Lin^- cells, we stained and sorted cells with anti-c-kit and anti-CD45 monoclonal antibodies and separated $CD45^+$ cells (region "A"). (C) Schematic illustration of the experimental design for analysis of in vivo enrichment of transduced hematopoietic cells.

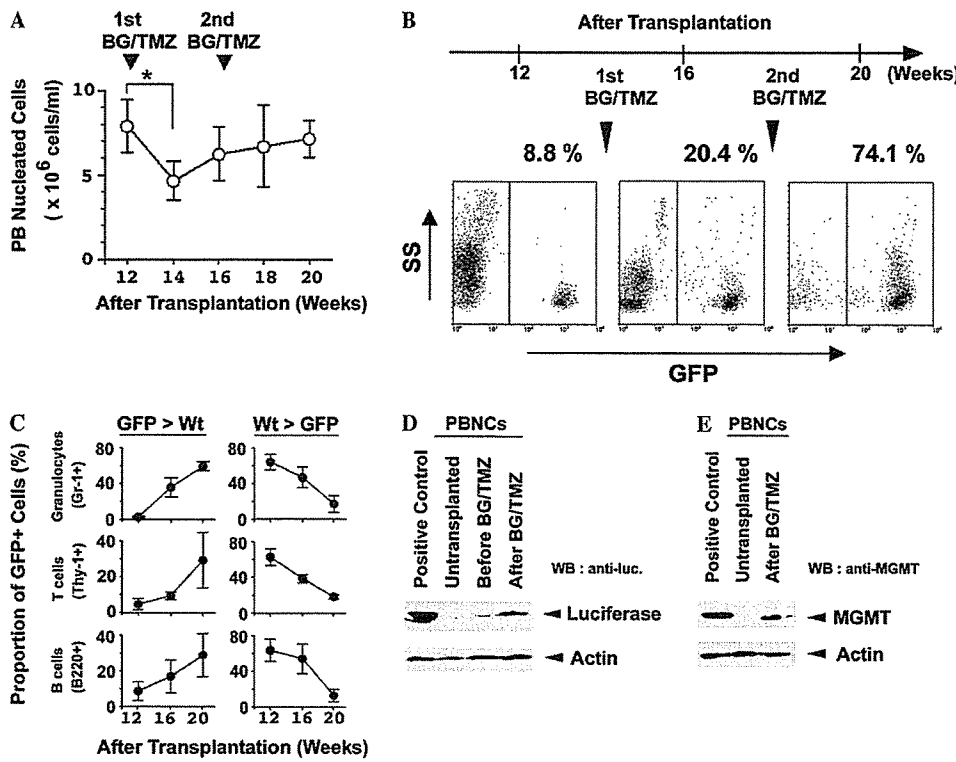

Fig. 3. In vivo enrichment of transduced hematopoietic cells. (A) PBNC counts during the treatment. Each circle and bar represents the mean value and standard deviation of 10 mice. *Statistically different ($P < 0.01$, unpaired Student t-test). (B) Proportion of transduced cells in PBNCs during the treatment. We examined the proportion of cells expressing GFP by a flow-cytometer. Data show one of representative mice. (C) Proportion of cells derived from donor mice in PBNCs during the treatment. We transduced $Lin^-/CD45^+$ cells of GFP-Tg or Wt mice by SF-luc/MGMT vector, transplanted into irradiated Wt or GFP-Tg mice (GFP > Wt or Wt > GFP, respectively (A)) and examined the proportion of cells expressing GFP in B220, Thy-1 or Gr-1-positive population by a flow-cytometer. Each circle and bar represents the mean value and standard deviation of three mice. (D) A luciferase protein and (E) a human MGMT protein in PBNCs of Wt > GFP mice were detected by Western blotting.

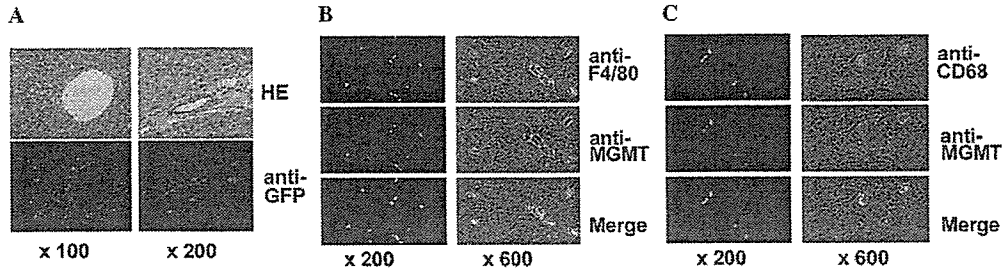

Fig. 4. Expression of a transgene in small cells along hepatic sinusoids in the liver of recipient mice (Wt > Wt). (A) Many small GFP+ cells were seen along hepatic sinusoids and several GFP+ cells in the wall of blood vessels (lower panels). The same slice of the liver was stained with hematoxylin–eosin (upper panels). (B) Expression of both F4/80 antigen and a transgene (MGMT) in small cells. (C) Expression of both CD68 and a transgene (MGMT) in small cells. [This figure appears in colour on the web].

(Fig. 5A). The latter cells were smaller than hepatocytes, were negative for endothelial marker, CD31 (data not shown), but positive for both a transgene, MGMT, and Kupffer cell markers, F4/80 [19] or CD68 [20] (Figs. 4B and C), indicating the expression of a transgene in Kupffer cells. To characterize the GFP+ cells in the liver more in detail, we stained the liver specimens of Wt > Wt mice with anti-MGMT and anti-albumin antibodies. While the small cells along sinusoid were positive for MGMT but not for albumin, a small number of large cells showed the immunoreactivity with both anti-GFP and anti-albumin antibodies (2–3 cells per one section, Fig. 5B). Thus, these large cells expressed both a donor-derived transgene, GFP, and a hepatocyte specific gene, albumin, although the proportion was very low (one cell per 10^5–10^6 hepatocytes). These results show that a FMEV-type vector provides an efficient transgene in the liver as well as HSCs in vivo.

To examine whether transduced HSCs transdifferentiate into albumin-positive cells or fuse with hepatocytes in vivo, we examined liver specimens of Wt > GFP mice. In these specimens, we also found that the large cells in the hepatic lobule (2–3 cells per one section) expressed a transgene, MGMT (Fig. 5C, left column), or luciferase (Fig. 5C, right column) and that these cells were also GFP-positive (Fig. 5C, middle and lower column). We could not find the cells which were GFP-negative and expressed MGMT or luciferase. These results indicate that a donor-derived MGMT-positive or luciferase-positive cells fused with recipient hepatocytes which were GFP-positive and synthesize albumin. Although the vectors provide efficient expression of a transgene in the liver, we could not find the evidence of transdifferentiation but the fusion of hematopoietic cells with hepatocytes.

4. Discussion

In this report, we showed that a FMEV-type vector provides a transgene expression in HSCs highly enough

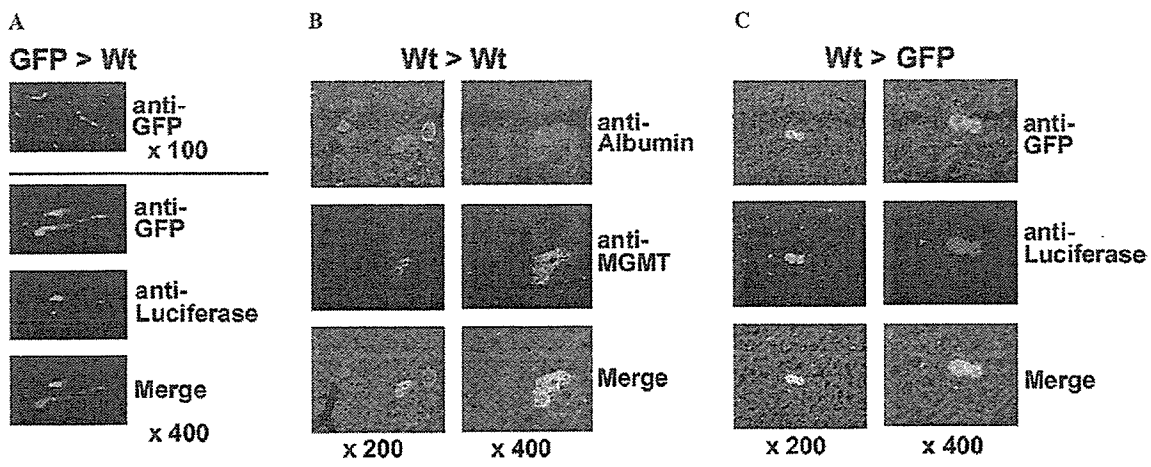

Fig. 5. Expression of transgenes in the liver. (A) Expression of a transgene, luciferase, in the liver of recipient mice (GFP > Wt). (B) Expression of a transgene, MGMT, in albumin-positive cells of recipient mice (Wt > Wt). (C) Expression of both a transgene (luciferase) and a recipient cell marker (GFP) in the liver of recipient mice (Wt > GFP). [This figure appears in colour on the web.]

to protect them from a DNA-methylating drug. Thus, this type of vector would be useful for the protection of HSCs from intensive chemotherapy toward cancers, such as hepatocellular carcinoma, and also for the enrichment of gene-modified HSCs in vivo. We also showed that even after the successful replacement of hematopoietic cells with transduced cells, these cells did not efficiently transdifferentiate into hepatocytes, suggesting that they rescued the injured hepatocytes temporarily through the fusion. Although we could detect fused cells, the proportion of these cells in the liver was extremely low (one cell per 10^5–10^6 hepatocytes). Recent study also demonstrated that the proportion of fused cells is rare in murine immune-mediated hepatitis model [21]. The low frequency of the fusion would suggest little therapeutic value, although fused cells expressed not only hepatocyte specific genes such as albumin but also a transgene of MDR. Thus transfer of a MDR gene into HSCs would enable the protection from myelosuppression but not the liver damage. Fused cells also suggest the possibility of the fusion events of hepatocellular carcinoma cells with hematopoietic cells expressing a drug-resistant gene. Such a fused cell would become a malignant cell which would be highly drug-resistant. Thus it should be very careful to transfer a MDR gene into HSCs in hepatocellular carcinoma patients.

Over past years, studies have been shown that stem cells of hematopoietic lineage can also transdifferentiate into nonhematopoietic tissue including the liver [10,11]. In contrast, some studies demonstrated that this so-called "plasticity of HSCs" appears to be rare event [22] and HSCs only fuse with hepatocytes in murine chemical hepatitis models [23,24]. Particularly, myelomonocytic cells are the source of hepatocytes fusion partner in murine model [25,26]. Our data are in good accordance with these reports, confirming them by a different approach.

Recent studies have revealed that multipotent adult progenitor cells [27] or unrestricted somatic stem cells [28] differentiate into hepatocytes in vivo. Human mesenchymal stem cells have been reported to differentiate into hepatocytes without fusion [29]. These cells but not HSCs would be good candidates as a target to achieve efficient protection of the liver from intensive chemotherapy or gene-modified long-term cell therapy for the liver.

Acknowledgements

We thank Prof. M. Okabe of Osaka University for providing us GFP-transgenic mice, TgN (β-act-EGFP)Osb. This work was partly supported by Grants-in-Aid from the Ministry of Education, Science, Sports and Culture of Japan.

References

[1] Mulligan RC. The basic science of gene therapy. Science 1993;260:926–932.
[2] Kay MA, Rothenberg S, Landen CN, Bellinger DA, Leland F, Toman C, et al. In vivo gene therapy of hemophilia B: sustained partial correction in factor IX-deficient dogs. Science 1993;262:117–119.
[3] Baum C, Hegewisch-Becker S, Eckert HG, Stocking C, Ostertag W. Novel retroviral vectors for efficient expression of the multidrug resistance (mdr-1) gene in early hematopoietic cells. J Virol 1995;69:7541–7547.
[4] Baum C, Itoh K, Meyer J, Laker C, Ito Y, Ostertag W. The potent enhancer activity of the polycytemic strain of spleen focus-forming virus in hematopoietic cells is governed by a binding site for Sp1 in the upstream control region and by a unique enhancer core motif, creating an exclusive target for PEBP/CBF. J Virol 1997;71:6323–6331.
[5] Tsuji T, Itoh K, Baum C, Ohnishi N, Tomiwa K, Hirano D, et al. Retroviral vector-mediated gene expression in human CD34+CD38− cells expanded in vitro: cis elements of FMEV are superior to those of Mo-MuLV. Hum Gene Ther 2000;11:271–284.
[6] Ohnishi N, Itoh K, Itoh Y, Baum C, Tsuji T, Nagao T, et al. High expression of transgenes mediated by hybrid retroviral vectors in hepatocytes: comparison of promoters from murine retroviruses in vitro and in vivo. Gene Ther 2002;9:303–306.
[7] Yamaguchi K, Itoh K, Ohnishi N, Itoh Y, Baum C, Tsuji T, et al. Engineered long terminal repeats of retroviral vectors transgene expression in hepatocytes in vitro and in vivo. Mol Ther 2003;5:796–803.
[8] Davis BM, Roth JC, Liu L, Xu-Welliver M, Pegg AE, Gerson SL. Characterization of the P140K, PVP(138-140)MLK, and G156A O^6-methylguanine–DNA methyltransferase mutants: implications for drug resistance gene therapy. Hum Gene Ther 1999;10:2769–2778.
[9] Williams DA, Hsieh K, DeSilva A, Mulligan RC. Protection of bone marrow transplant recipients from lethal doses of methotrexate by the generation of methotrexate-resistant bone marrow. J Exp Med 1987;166:210–218.
[10] Lagasse E, Connors H, Al-Dhalimy M, Reitsma M, Dohse M, Osborne L, et al. Purified hematopoietic stem cells can differentiate into hepatocytes in vivo. Nat Med 2000;6:1229–1234.
[11] Krause DS, Theise ND, Collector ML, Henegariu O, Hwang S, Gardner R, et al. Multi-organ, multi-lineage engraftment by a single bone marrow-derived stem cell. Cell 2001;105:369–377.
[12] Baum C, Eckert HG, Stocking C, Ostertag W. Activity of Friend mink cell focus-forming retrovirus during myelo-erythroid hematopoiesis. Exp Hematol 1996;24:364–370.
[13] Oumard A, Hennecke M, Hauser H, Nourbakhsh M. Translation of NRF mRNA is mediated by highly efficient internal ribosome entry. Mol Cell Biol 2000;20:2755–2759.
[14] Okabe M, Ikawa M, Kominami K, Nakanishi T, Nishimura Y. "Green mice" as a source of ubiquitous green cells. FEBS Lett 1997;407:313–319.
[15] Kitamura T, Onishi M, Kinoshita S, Shibuya A, Miyajima A, Nolan GP. Efficient screening of retroviral cDNA expression libraries. Proc Natl Acad Sci USA 1995;92:9146–9150.
[16] Markowitz D, Goff S, Bank A. A safe packaging line for gene transfer: separating viral genes on two different plasmids. J Virol 1988;62:1120–1124.
[17] Itoh K, Tezuka H, Sakoda H, Konno M, Nagata K, Uchiyama T, et al. Reproducible establishment of hemopoietic supportive stromal cell lines from murine bone marrow. Exp Hematol 1989;17:145–153.
[18] Higashitsuji H, Itoh K, Nagao T, Dawson S, Nonoguchi K, Kido T, et al. Reduced stability of retinoblastoma protein by gankyrin,